



Bioinspired interactive neuromorphic devices

Jinran Yu^{1,2}, Yifei Wang^{1,2}, Shanshan Qin¹, Guoyun Gao¹, Chong Xu^{1,2},
Zhong Lin Wang^{1,2,3,*}, Qijun Sun^{1,2,4,*}

¹ Beijing Institute of Nanoenergy and Nanosystems, Chinese Academy of Sciences, Beijing 101400, China

² School of Nanoscience and Technology, University of Chinese Academy of Sciences, Beijing 100049, China

³ School of Materials Science and Engineering, Georgia Institute of Technology, Atlanta, Georgia, 30332-0245, United States

⁴ Center on Nanoenergy Research, School of Physical Science and Technology, Guangxi University, Nanning 530004, China

The performance of conventional computer based on von Neumann architecture is limited due to the physical separation of memory and processor. By synergistically integrating various sensors with synaptic devices, recently emerging interactive neuromorphic devices can directly sense/store/process various stimuli information from external environments and implement functions of perception, learning, memory, and computation. In this review, we present the basic model of bioinspired interactive neuromorphic devices and discuss the performance metrics. Next, we summarize the recent progress and development of bioinspired interactive neuromorphic devices, which are classified into neuromorphic tactile systems, visual systems, auditory systems, and multisensory system. They are discussed in detail from the aspects of materials, device architectures, operating mechanisms, synaptic plasticity, and potential applications. Additionally, the bioinspired interactive neuromorphic devices that can fuse multiple/mixed sensing signals are proposed to address more realistic and sophisticated problems. Finally, we discuss the pros and cons regarding to the computing neurons and integrating sensory neurons and deliver the perspectives on interactive neuromorphic devices at the material, device, network, and system levels. It is believed the neuromorphic devices can provide promising solutions to next generation of interactive sensation/memory/computation toward the development of multimodal, low-power, and large-scale intelligent systems endowed with neuromorphic features.

Keywords: Neuromorphic devices; Synaptic transistors; Interactive; Neuromorphic computing; Bioinspired

Introduction

Brain is one of the most important organs of human body, supporting human vision, hearing, taste, smell, learning, memory, emotion, balance, and other perception related functions. The structure of brain is very complex, which consists of about 86 billion neurons connected by about 10^{15} synapses to form an extremely large and intricate biological neural network. The biological

neural network endows brain with powerful computing and learning capabilities, thereby enabling interactive perception and information processing between living creatures and environments with very low power consumption [1]. Even today's most powerful computers cannot compete with human brain when handling complex tasks of pattern recognition, risk management, or decision-making activities. This can be attributed to the following reasons. On one hand, traditional computers relying on von Neumann architecture have the processor unit and memory unit physically separated. Data moving back and forth between the processor and the memory consumes lots of

* Corresponding authors.

E-mail addresses: Lin Wang, Z. (zhong.wang@mse.gatech.edu), Sun, Q. (sunqijun@binn.cas.cn).

energy and time. So far, it has encountered the dilemma of energy efficiency bottlenecks in memory walls and the failure of Moore's law [2]. On the other hand, the analog sensing signals and digital computing signals are not compatible with each other to be processed together. As the number of sensor nodes increases, the raw data containing a large amount of redundant data has gradually become a huge burden for the sensory system [3,4]. Inspired by human brain and biological nervous system, how to design interactive neuromorphic chips to integrate sensing, storage, and processing capabilities, has become the dawn of breaking through von Neumann's bottleneck. The bioinspired interactive neuromorphic devices and systems are considered of great significance to endow intelligent Internet of Things with neuromorphic sensing and interactive characteristics in solving more complex realistic problems.

Fig. 1 shows the revolutionary shift in computing architecture from the von Neumann architecture to interactive neuromorphic computing. Unlike traditional computer processors, neuromorphic chips can simulate the functions and working patterns of human brain to handle more complicated tasks (e.g., somatosensory, image, and speech recognition). Hardware for neuromorphic computing utilizes the algorithm of artificial neural network (ANN) to emulate certain functions of the human brain by processing electrical pulse signals (analogy to the action potentials of biological neurons). To simulate human brain's ability of synchronizing parallel sensation information (e.g., touch, vision, and sound), the connections between artificial neurons can be readily updated through synaptic weights. This feature allows hardware to consume less energy and enables the processing speed of neuromorphic computation several orders of magnitude faster than that of conventional chips. The research and development of neuromorphic devices is considered one of the main tracks leading to the future era of

artificial intelligence. It is of great significance to investigate the solid-state devices/systems from the bottom architecture to emulate biological sensory synapses/neurons and develop ultra-low-power brain-like chips.

Biological nervous system

Inspired by biological nervous system, it is vital to design efficient neuromorphic devices with thorough understanding on the biological neurons, synapses, and brain functions. Human brain has 86 billion neurons (Fig. 2a) that receive and collect signals from a variety of stimuli and send the information to the designated areas of nervous system. The integration and interaction of vision, touch, hearing, smell, and taste in the human multisensory neural network facilitate high-level cognitive functionalities, such as information integration, recognition, reasoning, and imagination (Fig. 3a). In the human multisensory neural network, sensory receptors (e.g., rods and cones, mechanoreceptors, cochlea, smell receptors, taste receptors) can convert the physical information from ambient environment into potential changes and encode the potential changes into spike trains in the cell body using neural spike encoding. Subsequently, intermediate neurons transmit the spike trains from the receptors to the cerebral cortex in brain, where the information is decoded into sensory perceptions for further processing (Fig. 3b) [5]. When the sensory neurons receive stimulus input from receptors (or other neurons via dendrites), they can generate electrical signals and transmit them along axons to target neurons or muscles. The connection between an axon terminal and a dendrite on another neuron is called a synapse, which can be activated by action potential that reaches the axon terminal. The action potential allows calcium ions to enter the terminal, thereby activating cellular mechanisms to transport synaptic vesicles (full of neurotransmitters) to the presynaptic membrane. Neurotrans-

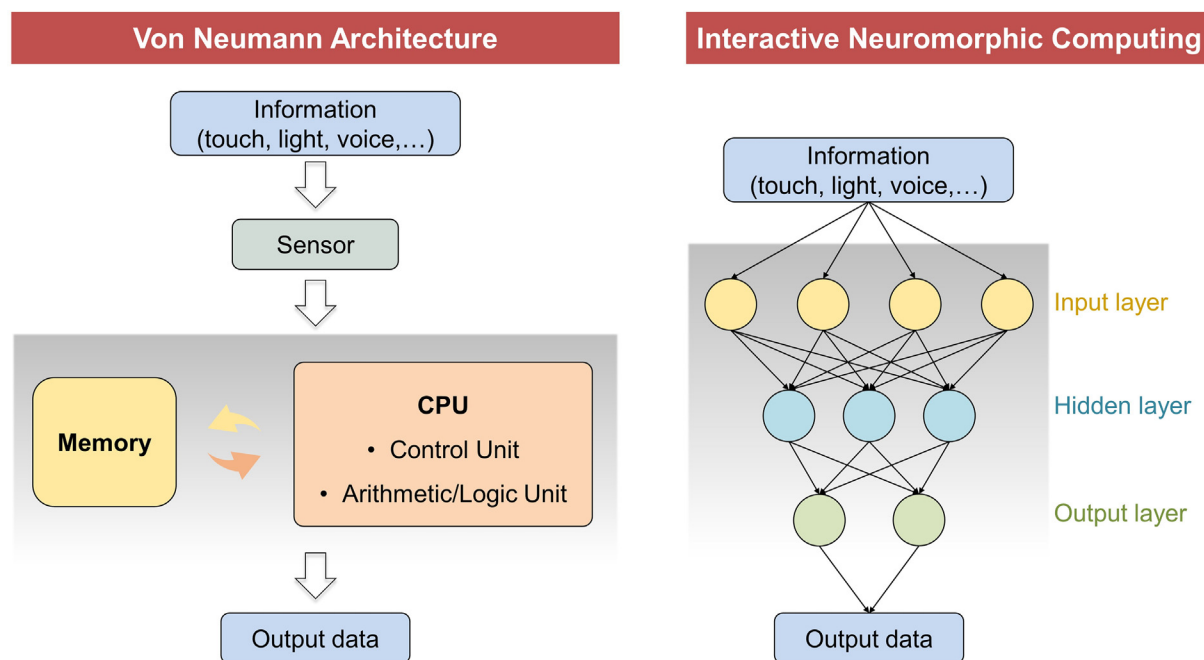


FIGURE 1

The revolutionary shift in computing architecture from the von Neumann architecture to bioinspired interactive neuromorphic computing.

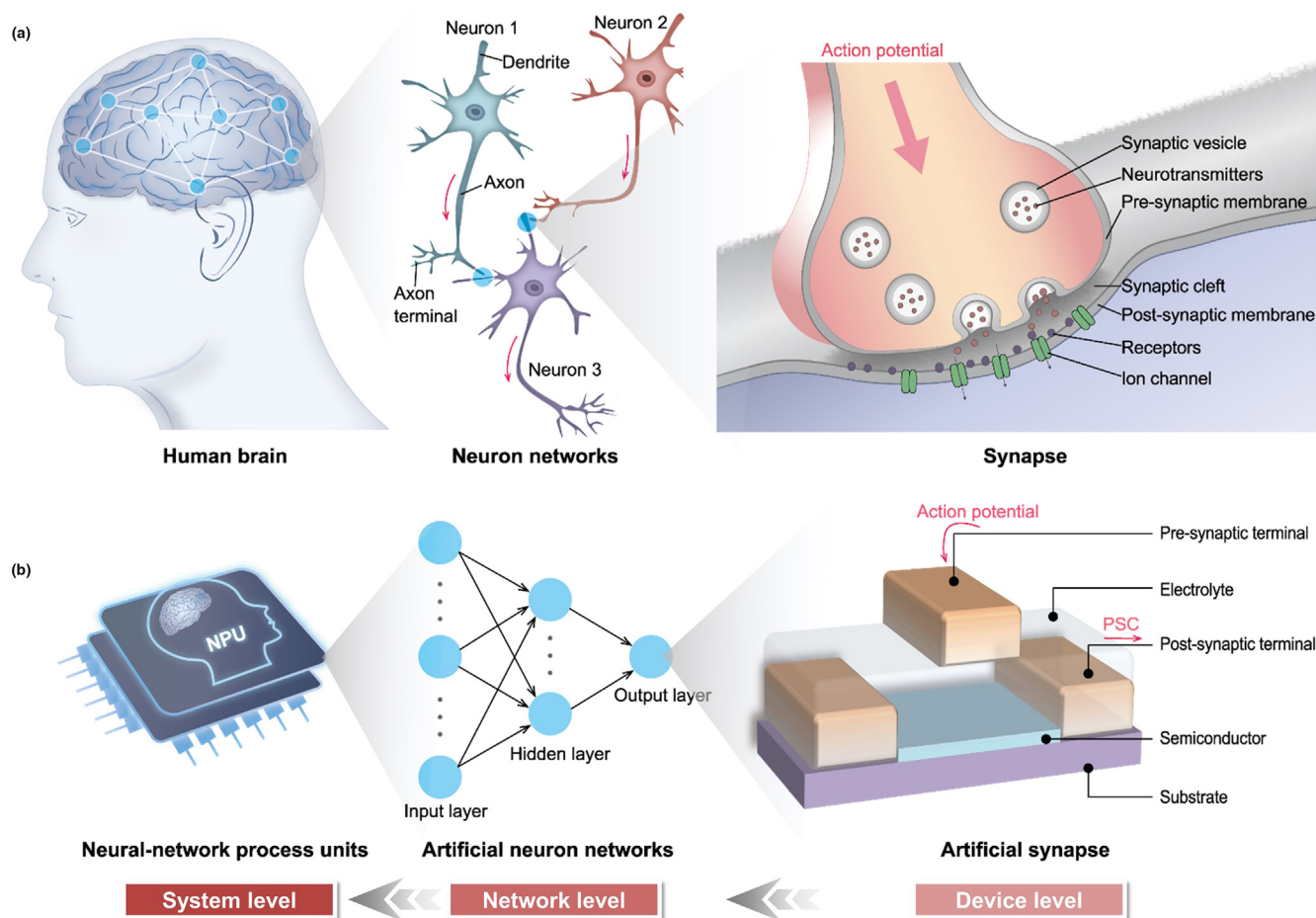


FIGURE 2

Comparison of human nervous system and bioinspired neuromorphic device. (a) Schematic diagrams of the human brain, neuron network, and synapse. The basic functional elements of neural networks are neurons and synapses. The transmission of action potentials via synapse is the basis of most communication in the nervous system. (b) Schematic diagrams of the neuromorphic chip, artificial neuron networks (ANNs), and artificial synapse. The neuromorphic chip is composed of different types of ANNs. The operation mechanism of these ANNs is related to two-terminal memristors or three-terminal transistors.

mitter molecules are then released into the synaptic cleft, which can diffuse throughout the synaptic cleft to activate (or bind to) the receptors on the postsynaptic membrane. Information transfer between neurons is primarily accomplished through the release of neurotransmitters from pre-synapse and the recognition of neurotransmitters on postsynaptic membrane. Transmission of action potentials via neurotransmitters is the basis of most communications in the nervous system (Fig. 3c) [6].

Bioinspired interactive neuromorphic device

Model of bioinspired interactive neuromorphic device

The basic model of neuromorphic device includes the following three progressive forms: simulation of neuronal activity at the device level, simulation of neural network connected by neuron-like devices at the network level, and simulation of the interactive sensation with external environment at the system level (Fig. 2b). The design and fabrication of artificial synapses and ANNs are inspired from the biological synapses and neural networks, respectively. In terms of terminal numbers, artificial synapses are usually divided into two-terminal devices and three-terminal devices. Their difference mainly lies in the path

of signal transmission and the means of weight modulation. For instance, the right panel in Fig. 2b shows a three-terminal synaptic transistor, which modulates the device conductance (i.e., synaptic weight) via an external electrode terminal. In detail, when an action potential reaches the presynaptic terminal (gate) to modulate ions migration/distribution in electrolyte, an electrostatic potential is induced to affect the channel conductance and results in a tunable postsynaptic current (between the source and drain).

Daily activities of human beings (e.g., thinking, learning, and action control) rely on the brain to receive information from inside and outside of the body. Various information is transmitted through the biological nervous system, which constitutes the five basic senses of sight, hearing, smell, touch, and taste, as well as the basic functional systems of somatosensory system, vestibular system, internal sensory system, etc. The developed synaptic devices in early days mainly use electrical pulse as a stimulus signal, which are lack of emulation on various sensory behaviors. To emulate a more realistic nervous system, it is necessary to explore the effect of sensory signals on the updating process of synaptic weights. How to further implement sophisticated weight-updating through multiple/mixed sensory mode is

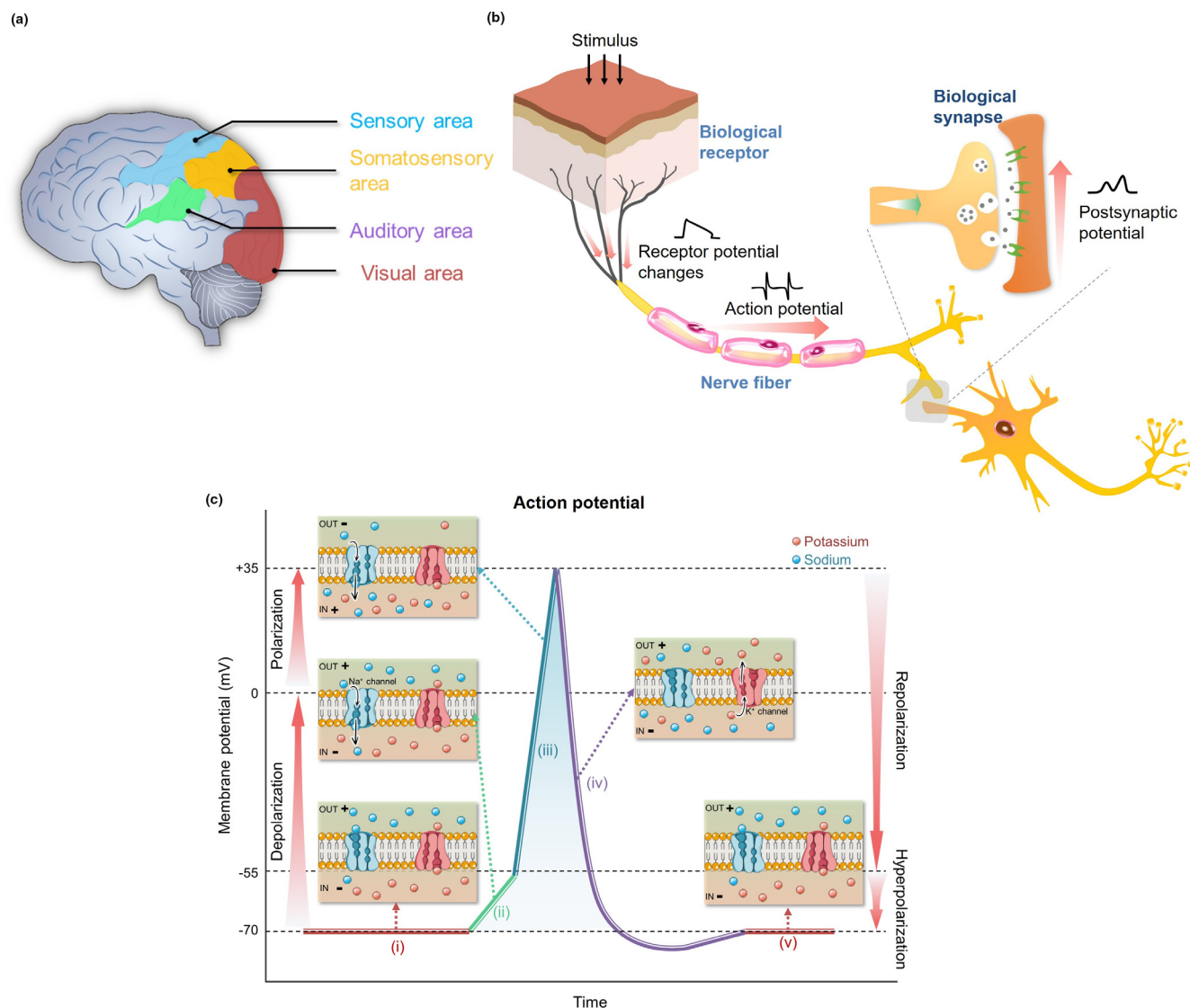


FIGURE 3

(a) Biological multisensory system. (b) A biological afferent nerve. Stimulus applied to receptors change the potential of each receptor. The receptor potentials combine and initiate action potentials at the heminode. Nerve fibers form synapses with interneurons. Action potentials from multiple nerve fibers combine via synapses to facilitate information processing. (c) Action potential and schematic diagram of ion exchange mechanism. (i) In the resting state, potassium ions dominate the cell membrane, and the equilibrium potential is negative. (ii) Sodium channels are activated by excitatory neurotransmitters, prompting sodium ions to flow into the membrane. (iii) More sodium channels are activated when the membrane potential increases to a certain threshold, resulting in a short, large voltage spike. The region with the membrane potential rising from -70 to 0 mV defines the depolarization process. When the membrane potential further increases from 0 to $+35$ mV, the membrane potential becomes internally positive and externally negative, forming the polarization process. (iv) When the sodium channel is closed and the potassium channel is opened, the membrane potential returns to the negative potassium equilibrium state, i.e., repolarization. (v) All channels are reset and the cells return to resting state dominated by potassium ion. Due to the increase of negative charge in the membrane, the voltage is usually lower than the resting potential. The membrane potential dropping below -70 mV can be attributed to the remaining-opened potassium channels, which allow more potassium ions to diffuse out of the membrane and lead to the negative membrane potential. This process is also known as hyperpolarization.

also an urgent issue. A bioinspired interactive neuromorphic device typically includes a bionic receptor integrated with an artificial synapse. The bionic receptor is used to perceive external stimuli (e.g., pressure, sound, light, and heat) and convert the stimuli into electrical signals (i.e., the input action signals transmitted to the presynaptic terminal of artificial synapse). After receiving the action signal from the bionic receptor, the synaptic device is activated to generate a postsynaptic current (Fig. 4a).

Bionic receptor

To achieve the interactive neuromorphic devices, different types of bionic receptors are primarily required to emulate various biological receptors (Fig. 4b). For instance, the main types of bionic mechanoreceptors can be designed based on resistive, capacitive, piezoelectric, and triboelectric sensors. Bionic mechanoreceptors are analogous to biological mechanoreceptors located on the skin (e.g., ring corpuscles and Merkel's discs), which can sense

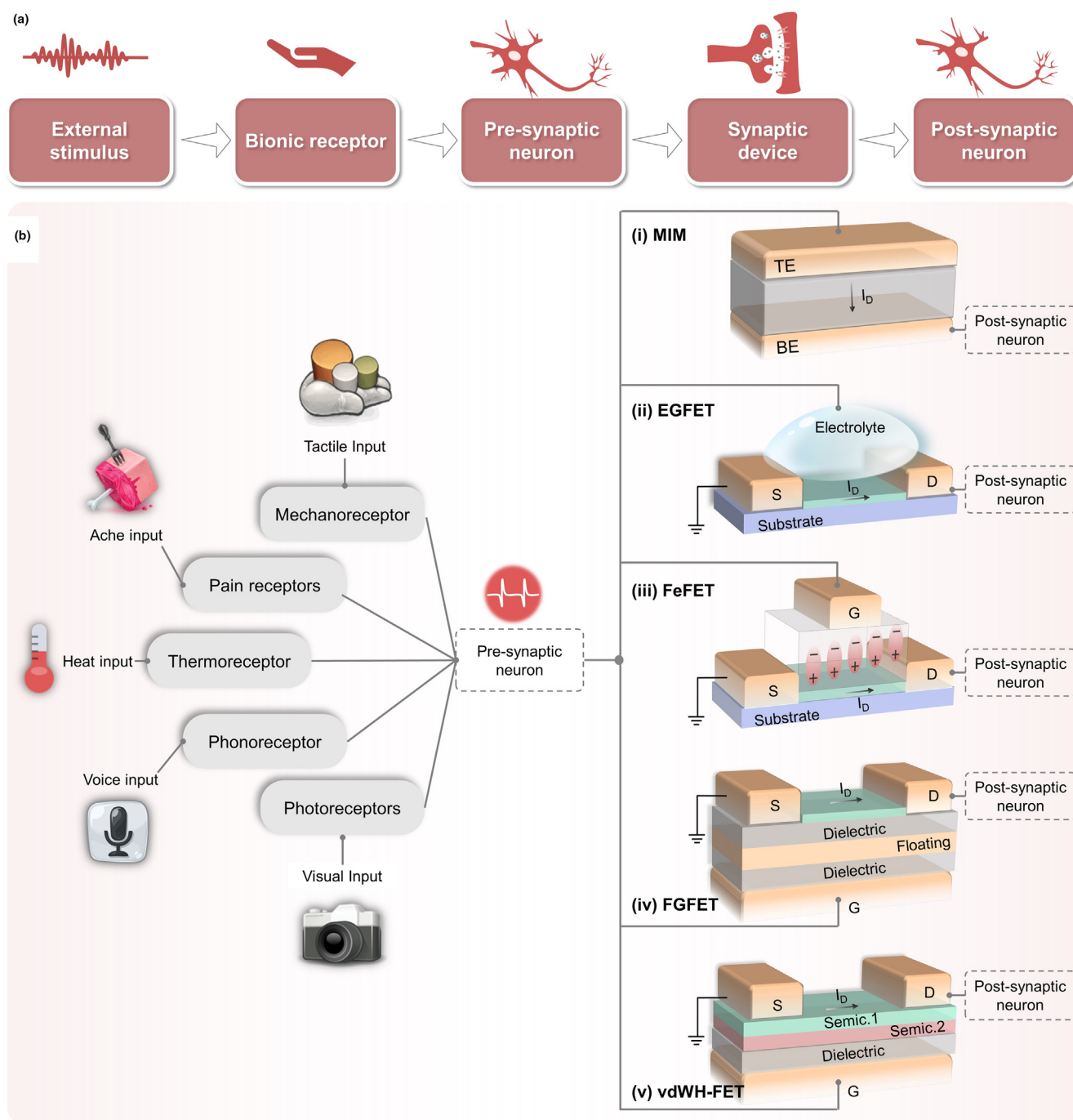


FIGURE 4

(a) Schematic diagram of the signal processing steps of the bioinspired interactive neuromorphic devices. (b) Schematic Illustration of various bioinspired interactive neuromorphic devices. (i) MIM structure. (ii) EGFET structure. (iii) FeFET structure. (iv) FGFET structure. (v) vdW heterostructure FET structure.

mechanical signals of pressure, touch, stretch, and vibration. Bionic pain receptors are mainly chemical sensors and are analogous to biological chemical receptors. This type of receptor is used to simulate the unpleasant feeling when the body is subjected to noxious stimuli. Bionic thermoreceptors are mostly thermoelectric devices which can be used to simulate the body's response to temperature changes. Bionic phonoreceptors are used to emulate the function of cochlea to detect the vibratory stimuli, which are further incorporated with synaptic devices to mimic the sense

of hearing by simulating nerve impulses and transmitting them to the artificial auditory centers of the cerebral cortex. Bionic visual receptors can be used to emulate the function of retina to detect visual signals and construct complex visual systems. Optoelectronic synaptic devices based on photoconductive materials can be used to simulate typical behaviors of photonic synapses and fabricated into visual sensor array (or ANNs) to implement image recognition, simulate artificial adaptive retinas, etc. [7–14].

Artificial synapse

Biological synapses are characterized by plasticity that controls the strength of connections between neurons (i.e., synaptic weight), which is the basis for biological systems to achieve learning, reasoning, and other intelligent functions [15]. In ANN, the connections between neurons are also constructed based on a mathematical model of synaptic plasticity. Inspired by the weight-updating process (i.e., conductance modulation) in biological synapses, artificial synapses utilize the readily tunable conductivity in novel electronic materials to simulate the typical electrical characteristics of biological synapses. In recent years, various electronic devices have been constructed to simulate synaptic plasticity, which is expected to be a breakthrough and promising means to neuromorphic engineering and computation. Two-terminal memristors with point-to-point connection properties have been extensively studied as neuromorphic devices [16–22]; three-terminal synaptic transistor showing point-to-line properties are also emerging to simulate synaptic functions and emulate sensory neurons [23–30]. Three-terminal transistors are quite different from two-terminal memristors as it uses different channels for signal-transmitting (source to drain) and weight-updating (gate to source). Optional device architectures can be used for three-terminal synaptic transistors, including electrolyte-gated transistor, ferroelectric transistor, floating-gate transistor, and van der Waals heterostructure transistor (Fig. 4b). Based on the intrinsic properties of active materials (e.g., piezoelectric, triboelectric, optoelectronic, thermoelectric, electrochemical, and phase transition), two-/three-/multi-terminal synaptic devices can be readily designed by appropriate material selection and structural design. Bionic receptors can also be systematically integrated to link external physical stimuli (pressure, vibration, light, temperature, etc.) with neuromorphic electrical signals, realizing direct interaction between external environment and artificial synapses (or afferent nerves) [13,29,31,32], i.e., bioinspired interactive neuromorphic devices.

Memristor

The progressively precise synthesis methods of nanoscale materials and paired nanofabrication techniques have facilitated the development of memristors [33]. Memristors generally use a typical metal–insulator–metal (MIM) structure with the insulator layer sandwiched by two metal electrodes (Fig. 4b-i) [18,33]. High resistance materials (e.g., metal oxides [34–36], chalcogenide materials [37], 2D transition metal dichalcogenides (TMD) [38], perovskites [39–42], and heterostructures [43]) are usually used as the insulating layer of memristor. The working mechanism of memristor relies on the transition between high resistance and low resistance states caused by the formation of conductive filament or the phase change of insulating materials [17]. Memristors have become an important candidate for synaptic devices in neuromorphic chips due to their continuously adjustable resistance, non-volatile information storage, low power consumption, high integration, etc.

Electrolyte-gated synaptic transistor

To meet the key requirements for low power consumption in synaptic devices, there is an urgent need for devices to operate in low voltage. Device engineering on dielectric layers with

ultra-high capacitance has attracted considerable attentions [44]. An electrolyte gate field-effect transistor (EGFET) is a typical low-voltage-operating device that uses the coupling effect between the ions in the electrolyte and the charge carriers in the semiconductor to realize effective modulation on channel conductance [45,46]. In general, electrolyte-gated transistors can be classified into two categories depending on whether ions react with the semiconductor material, including electrostatically controlled electric double layer FETs (EDL-FETs) and electrochemical FETs [47]. The migration of ions in the electrolyte gate under an applied electric field can readily simulate the response of neurotransmitters to action potentials, which has significantly contributed to the research on neuromorphic devices in recent years. The gate electrode and semiconductor channel of EGFET are analogous to the presynaptic terminal and postsynaptic membrane, respectively (Fig. 4b-ii). The EDL-FET based synaptic devices mainly cover organic semiconductor [44,48], oxide [8,49–51], or 2D semiconductor [52] transistors controlled by ionic liquid or proton conductor, relying on the formation of EDLs at the interfaces of semiconductor channel/electrolyte and gate electrode/electrolyte [53]. The electrochemical FET based synaptic devices implement gate modulation based on the redox reaction of a modified semiconductor (e.g., poly(3,4-ethylenedioxythiophene)/poly(styrene sulfonic acid), PEDOT:PSS). In this way, the emulation of neural signals can be realized at ultralow operating voltages, thereby reducing the power consumption of a single spike in the artificial neuron [54]. Besides, ion-controlled synaptic devices based on the intercalation and delamination of lithium ions in 2D semiconductor materials can also induce the conductance changes in transistor channels, which have recently been widely used in artificial synapse studies [28,38].

Ferroelectric-gated synaptic transistor

A ferroelectric field-effect transistor (FeFET, Fig. 4b-iii) is a type of storage device that uses ferroelectric insulators (e.g., bulk perovskites [55], doped hafnium oxides [56], and piezoelectric copolymers [57]) as gate dielectrics, exhibiting non-volatile, low-power-consuming, and high-speed writing/erasing properties [58]. Early industry attempts at ferroelectric devices based on perovskite-structured composite oxide ferroelectrics. Until 2011, the discovery of ferroelectricity in fluorite-structured binary oxides (e.g., hafnium oxide, HfO₂) have revived the research enthusiasm in FeFET for advanced microelectronics and modern semiconductor industry [59,60]. According to the reversible remanent-polarization in the ferroelectric insulating layer, the threshold voltage and channel conductance of the FeFET can be readily modulated by varying the gate voltage to change the polarization state of ferroelectric dielectrics [27,46,61]. The purely electrical modulation on channel conductance through ferroelectric polarization has also received extensive attentions to simulate typical synaptic properties (e.g., long-term potentiation/depression and spike-timing dependent plasticity), which can enable both functions of information processing and storage [62]. Although the retention time of conventional FeFETs is limited due to the presence of charge traps and gate leakage currents, recently emerging 2D ferroelectric materials can potentially solve these problems because the polarization process of the device

occurs in the channel material itself rather than within the gate dielectrics [63]. 2D ferroelectric materials also exhibit robust ferroelectricity and nonvolatile memory properties without annealing at room temperature [63,64]. Furthermore, 2D layered ferroelectric semiconductors have the potential for continuous size reduction in atomic thickness, which are highly promising for future high-density integration and neuromorphic computing [64].

Floating-gate synaptic transistor

Floating-gate field effect transistor (FGFET) shows a similar structure to conventional transistor, but has an additional layer of floating gate embedded in dielectrics (Fig. 4b-iv) [65]. Conventional FETs typically exhibit volatile behavior due to the rapid dissipation of the accumulated charges in channel when the gate voltage disappears. For FGFET, the floating-gate can be considered as a charge trapper, which deliver a shielding effect to the applied gate voltage, thus retaining the channel conductance and providing long-term storage performance [65]. This non-volatile storage characteristic facilitates the simulation of long-term plasticity behavior of synapses [10,66]. However, high operating voltages (~ 20 V) and long response time (10–100 ms) are required for information writing/erasing and data storage, which limits the extensive development of FGFETs. When device size gets closer to the physical limit, the industry urgently calls for new structures and new principles of transistors and memories to gain the improvements on operation speed, integration density, and power consumption. Recently, semi-floating-gated FETs (SFGFETs) have been successfully designed with low operating voltage, large threshold window, and ultra-high-speed writing process (in nanoseconds) [67–69]. In the SFGFET, a p-n junction diode is formed between the floating gate and the drain to constitute a tunneling FET, which thereby makes the floating gate turn to semi-floating geometry. Thus, four regions are formed in the SFGFET, including drain, source, control gate, and semi-floating gate [69]. The reported SFGFET mainly relies on complementary metal–oxide semiconductor (CMOS) technology or van der Waals heterostructure technology. By manipulating the type and density of charge carriers in the semi-floating gate, the channel conductance can exhibit non-volatile and continuous variation. This type of devices has also been shown to have the potential to emulate advanced neuromorphic computing with ultrahigh speed and long refresh time [68,70].

vdW heterostructure synaptic transistor

In 2D material family, layered materials are readily stacked by van der Waals (vdW) force to form vdW heterostructures. Transistors based on this structure are defined as vdW heterostructure transistors [71]. In vdW heterostructures, the combination of 2D materials with different band gaps can lead to some unique physical properties (electrical or optical properties), which can be used to simulate special synaptic behaviors (Fig. 4b-v). For examples, the tunable electrical properties of heterostructure between black phosphorus (BP) and tin selenide (SnSe) are used to simulate different states of synaptic connection, where excitatory and inhibitory postsynaptic currents can be dynamically reconstructed [72]. By exploiting the gate-tunable and persistent photoconductivity of graphene and MoS₂ heterostructures [73,74], a

mechano-photonic artificial synapse based on graphene/MoS₂ heterostructure is realized [13]. The vdW heterostructure concept can also be extended to the combination of 2D materials with other functional materials in different dimensions [75], e.g., hybridized quantum dots [76], nanowires/nanotubes [77], thin-film semiconductors [78], etc. The enormous family of heterostructures is highly promising for enriching the synaptic devices with versatile functionalities. In addition, the participation of 2D layered materials provides a more flexible and convenient approach to on-demand design of neuromorphic devices. Extensive investigation on 2D vdW heterostructures may pave the way to breaking through Moore's law and achieving high-performance electronic devices with reconfigurability, versatility, and flexibility.

Figure of merits

Comprehensive evaluating the figure of merits for interactive neuromorphic devices is of great significance to improve the sensing activity, interactive efficacy, learning accuracy, and energy efficiency. The desirable characteristics are mainly discussed from the aspects of synaptic plasticity, energy consumption, dynamic range, linearity and symmetry, and stability and reliability.

Synaptic plasticity

Generally, synaptic plasticity can be divided into short-term plasticity (STP) and long-term plasticity (LTP). The STP is activated by transient stimuli and capable to recover in a short time, which can be reflected in two typical behaviors of paired-pulse facilitation (PPF) and paired-pulse depression (PPD). PPF refers to an increase in PSC evoked by a second spike when the second spike immediately follows the previous one. PPF is considered to be important for the decoding of temporal information in biological systems [79,80], which can be evaluated by PPF index (A_2/A_1 , where A_1 and A_2 represent the amplitudes of the first and second PSCs, respectively) [81]. In contrast, the LTP evoked by unremitting or multiple stimuli shows persistent facilitatory or inhibitory effects, manifesting long-term potentiation or depression behaviors. The exhibited LTP behavior is mainly determined by the weight updating mechanism used for ANN simulations (discussed later in Fig. 7) [15]. The basic principle of synaptic plasticity is described by Hebbian Rule proposed by Hebb in 1949, which indicates that successive (or repeated) stimulation on postsynaptic neurons by presynaptic neurons can lead to enhanced synaptic transmission efficiency [82]. Based on this theory, the spike-timing dependent plasticity (STDP) learning method proposed in 1997 describes how to adjust the strength of connections between neurons according to their learning orders [83,84].

Energy consumption

As the energy dissipation of biological synapses is close to 10 fJ, it is essential to reduce the energy dissipation of artificial synapses. In biological synapses, the spike voltage is ~ 10 mV, the ionic current is ~ 1 nA, and the spike period is ~ 1 ms, resulting in an energy of about 10 fJ [85]. The energy dissipation (E) of a single spike event is determined by the peak current of conductive channel (I_{peak}), the drain voltage (V_D), and presynaptic-spike

duration (t), which can be calculated as $E = V_D \times I_{\text{peak}} \times t$. Accordingly, further device engineering is needed to reduce energy consumption, e.g., accelerating the writing speed to \sim ns [68,86] or reducing the operating voltage to \sim mV [48,87] while maintaining its conductance modulation properties.

Dynamic range (on/off ratio)

The dynamic range is defined as the on/off ratio of the maximum conductance to the minimum conductance ($G_{\text{max}}/G_{\text{min}}$), which is used to describe the total modulation range by synaptic devices [88]. Larger on/off ratio implies better mapping capability of the synaptic weights in the algorithm to the device conductance. This is because the synaptic weights in the algorithm are commonly normalized over a range between 0 and 1 [85].

Linearity and symmetry

The linearity refers to the extracted linearity from the curve of synaptic device conductance vs input pulses number (or the number of stimuli), which should be linear in the ideal circumstance. Symmetry refers to the curve symmetry between the trajectory of conductance-increasing process (potentiation) and the trajectory of conductance-decreasing process (depression). In most cases, the weight updating curves of either two-terminal or three-terminal synaptic devices exhibit nonlinearity and asymmetry, which will inevitably cause the reduction in the learning accuracy of artificial neural networks. Changing the pulse input regime can help to attenuate this effect, but it may aggravate the processing burden of sensor unit and peripheral circuitry [33,85,88–90].

Stability and reliability

Stability and reliability are critical for the on-chip integration of bioinspired interactive neuromorphic devices, in terms of both the cyclic stability of each unit (sensor and synaptic devices) and the device-to-device reliability. Random variations in conductivity due to the instability and unreliability of each unit may raise the risk of degradation in computing capability and learning accuracy for the integrated chip.

Fig. 5 shows the timeline of milestones in pursuing bioinspired interactive neuromorphic devices. In this review, we summarize the recent progress and development of bioinspired interactive neuromorphic devices, which are classified into neuromorphic tactile systems, visual systems, auditory systems, and multisensory systems. They are discussed in detail from the aspects of materials, device architectures, operating mechanisms, synaptic plasticity, and potential applications. Additionally, the bioinspired interactive neuromorphic devices that can fuse multiple/mixed sensing signals are proposed to address more realistic and sophisticated problems. Finally, we deliver the perspectives on interactive neuromorphic devices at the material, device, network, and system levels. It is believed the neuromorphic devices can provide promising solutions to next generation of interactive sensation/memory/computation toward the development of multimodal, low-power, and large-scale intelligent systems endowed with neuromorphic features.

Bioinspired neuromorphic tactile system

The cooperation of receptors, neurons, and synapses in the somatosensory system allows for effective recognition and processing on complex tactile information [31]. Physiologically, the tactile signals are detected by mechanoreceptors on the skin. As shown in Fig. 6a, the tactile stimuli signals are transmitted along a long string of axons through synapses to postsynaptic neurons for further processing and recognition on the tactile information [91,92]. The skin of organisms is covered with different types of mechanoreceptors that are used to record specific types of tactile stimuli and to perform the function of pressure and touch recognition. For example, pressure receptors are mainly composed of Pacinian corpuscles, which are fast adaptive receptors used to perceive pressure. Touch receptors mainly consist of Meisner bodies, Rufini bodies, and Merkel discs, which are usually slowly adaptive receptors used to perceive touch information [93]. According to different working mechanisms, the bionic mechanoreceptors can be classified into resistive, capacitive, piezoelectric, and triboelectric sensors. Resistive and capacitive mechanoreceptors can sense continuous static forces, while piezoelectric and triboelectric mechanoreceptors can sense instantaneous dynamic pressures [94].

Table 1 summarizes the bioinspired neuromorphic tactile systems (NTS) activated by artificial bionic mechanoreceptors, including capacitive-NTS, resistive-NTS, piezoelectric-NTS, and triboelectric-NTS. As a specific category, the EDL-NTS is discussed in Section “EDL structure based neuromorphic tactile system”. The artificial reflex arc and adaptive systems in a more complete form are discussed in Section “Artificial reflex arc”.

Capacitive neuromorphic tactile system

Regarding to the primary requirements for pressure/strain/tactile sensation in NTS, it is a challenge to building efficient devices by integrating pressure sensing components and signal processing units. Recently, a capacitive pressure sensor based on organic field-effect transistor (OFET) with high sensitivity ($8\text{--}192\text{ kPa}^{-1}$) has been well developed to emulate the functions of biological mechanoreceptor [44,95]. Integrating the pressure sensory OFET (capable of sensing instantaneous pressure stimulation) with another organic synaptic transistor to form a dual-OFET-based synaptic device is a pioneering study toward capacitive neuromorphic tactile system. The capacitive-NTS is composed of a capacitive mechanoreceptor with pressure sensing function and a proton conductor gated synaptic transistor with signal processing function, achieving the functional fusion of signal transduction and information processing. Fig. 6b shows the simplified schematic diagram of a capacitive-NTS. The capacitance of the pressure sensor varies with the applied external pressure and is converted into a pulsed electrical signal that is transmitted through the gate to the presynaptic terminal of the second organic synaptic transistor. When the presynaptic terminal receives the pulse signal, the migration of protons in the dielectric layer affects the accumulation state of charge carriers in the organic semiconductor channel. As a result, the postsynaptic current (PSC) will be modulated across the source and drain electrodes. The characteristics of the PSC response depend on the amplitude, frequency, and duration of the applied pressure.

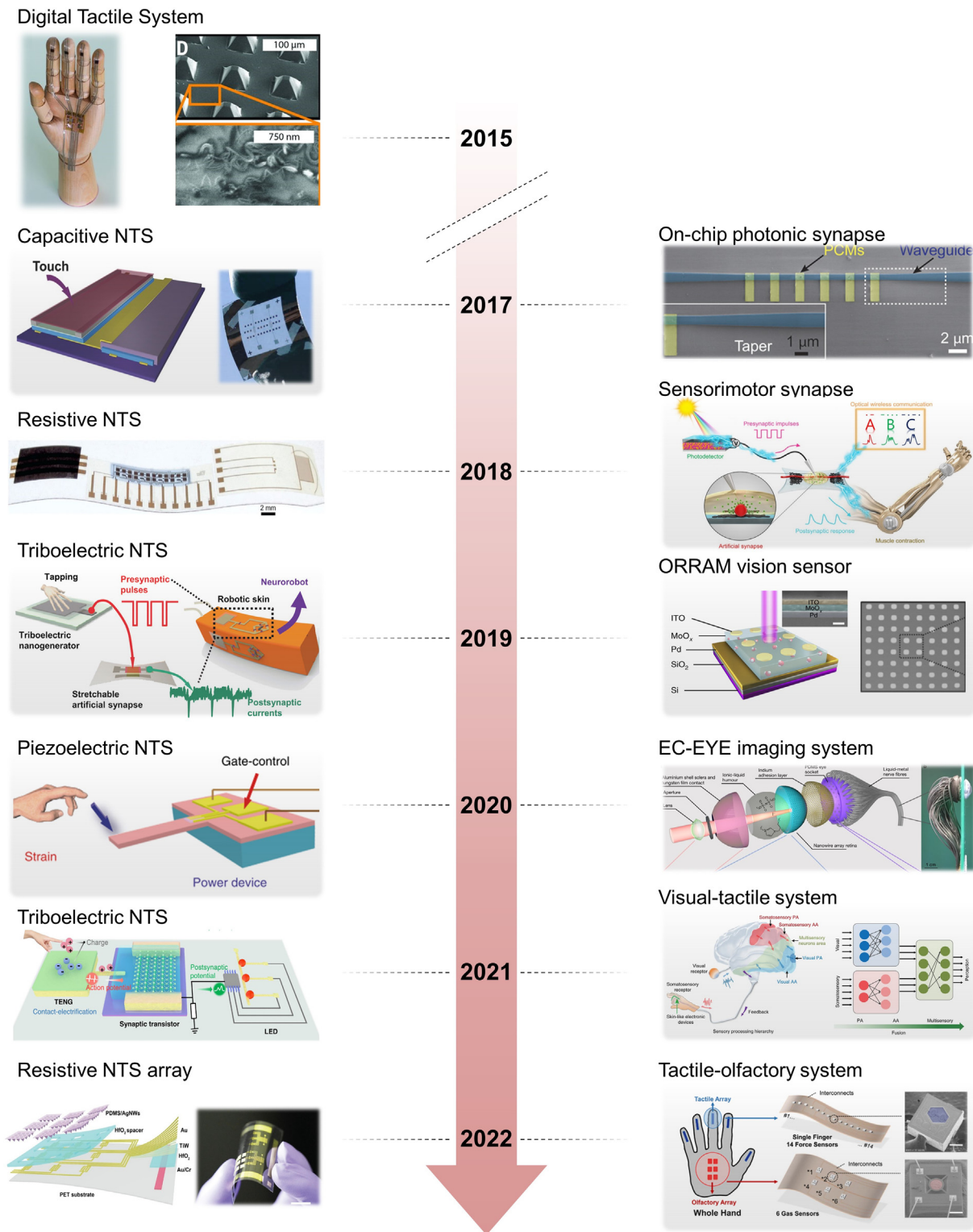


FIGURE 5

Timeline of milestones for pursuing bioinspired interactive neuromorphic devices.

Therefore, by detecting the change of PSC in the capacitive-NTS, dynamic pressure signals, time-dependent characteristics, and comprehensive tactile information can be collected and analyzed. The capacitive-NTS provides a reference to the compatible integration of pressure sensors and intelligent devices with synaptic functions [44].

Resistive neuromorphic tactile system

Neuromorphic tactile processing unit based on resistive pressure sensor and synaptic device is proposed to integrate and distinguish the temporal and spatial characteristics of touch signals. Typical resistive-NTS consists of a resistive pressure sensor and a synaptic device, corresponding to the sensory receptors and

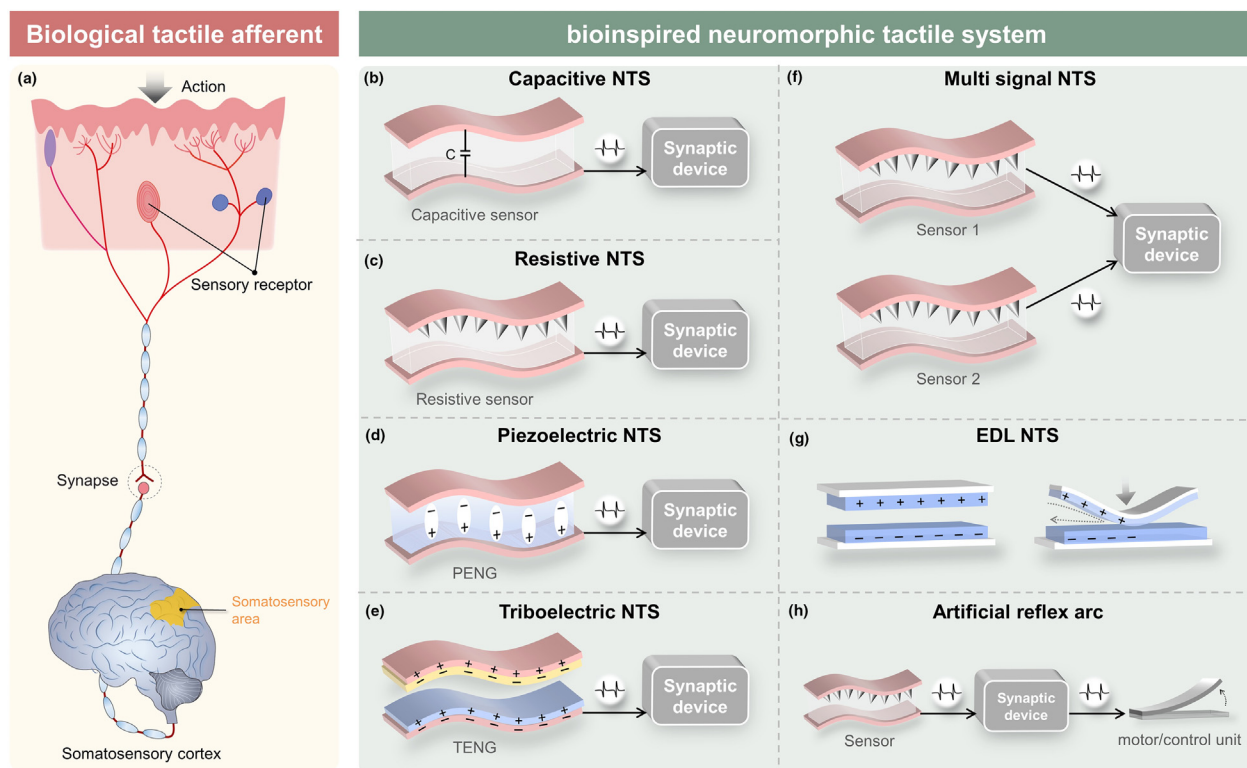


FIGURE 6

Biological tactile afferent nerve and bioinspired neuromorphic tactile system. (a) Schematic diagram of biological tactile afferent nerve. (b) Capacitive NTS: a capacitive pressure sensor activated artificial synaptic device. (c) Resistive NTS: a resistive pressure sensor activated artificial synaptic device. (d) Piezoelectric NTS: a PENG activated artificial synaptic device. (e) Triboelectric NTS: a TENG activated artificial synaptic device. (f) Multi-signal NTS: two or more sensors activated artificial synaptic device. (g) EDL structure activated neuromorphic tactile system (EDL-NTS). (h) Artificial reflex arc.

TABLE 1

Summary of bioinspired neuromorphic tactile systems (NTS).

NTS structure	Mechanoreceptor	Synaptic device			Synaptic behavior	Refs.
		Structure	Active material	Dielectric material		
Capacitive-NTS	OFET-based sensor	EGFET	PDPP3T	Chitosan	Tactile-perception	[44]
	-	EDL structure	Graphite	-	Multi-point stimulation	[111]
Resistive-NTS	CNT sensor/Ion cable	EGFET	IWO	PVA	Tactile pattern recognition	[92]
	CNT sensor/Oscillator	EGFET	Conjugated polymer	Ion gel	Braille recognition, reflex arc	[31]
	Rubber-based sensor	EGFET	P3HT-NF	Ion gel	PPF, STP, LTP	[99]
Piezoelectric-NTS	PDMS/AgNWs sensor array	Memristor array	Au/TiW/HfO ₂ /Au	-	Near-sensor computing	[100]
	Polymer-based PENG	EGFET	Graphene	Ion gel	EPSC, IPSC, PPF, dynamic logic	[29]
	GaN-based PENG	Heterostructure	AlGaN/AlN/GaN	-	Human reflex	[104]
Triboelectric-NTS	-	Heterostructure	NiO/ZnO	-	PPF, STDP, spatiotemporal tactile sensing	[184]
	TENG	FGFET	MoS ₂	HfO ₂	PPD/F, STP/LTP, dynamic logic	[66]
	TENG	FeFET	Pentacene	BT/P(VDF-TrFE)	STP/LTP	[110]
	TENG	EGFET	MoS ₂	Ion gel	EPSC, PPF, spatiotemporal tactile sensing	[32]
	TENG	EGFET	P3HT-NF	Ion gel	Neurobot locomotion	[99]
	TENG	EGFET	PDVT-10	Ion gel	EPSC, PPF, STP to LTP, dynamic logic	[185]
TENG	EGFET	MoS ₂	Proton conductor	EPSC, PPF	[109]	

information-processing synapses in biological system, respectively (Fig. 6c). The resistive pressure sensor is used as bionic mechanoreceptor, whose function is to convert pressure stimuli into electrical signals and transmit them to the presynaptic terminal of the synaptic device.

Pyramid-micro-structured polydimethylsiloxane (PDMS) coated with a conductive layer has been extensively investigated as the active sensing unit for pressure sensor [31,96–98]. Chen's group [92] designs a resistive-NTS composed of a carbon nanotube (CNT) based micro-structured resistive pressure sensor, an ionic cable, and an electrolyte gated indium tungsten oxide (IWO) transistor. When an external force is applied on the pressure sensor, the induced resistance change causes a voltage drop across the ionic cable. The voltage drop will cause different voltage pulse signals to be transmitted to the transistor channel and implement field-effect modulation. The strong electrical field induced by ion migration adjusts the charge carrier density in the channel, resulting in the PSC response. When the pressure is maintained, more ions are accumulated at the interface, which enhances the amplitude of PSC. After the pressure is released, the voltage drop on the ionic cable will suddenly decrease, the ions will gradually drift back to their equilibrium positions, and the PSC will gradually return to the initial level. Based on the electrical response of the resistive-NTS to external stimulation/attenuation signal, the applied tactile characteristics can be recognized and extracted.

In 2018, scientists have integrated a CNT-based pressure sensor with an OFET-based oscillator to form an artificial afferent nerve [31]. This structure design has the advantage that the pressure signals are directly converted into voltage signals with frequency characteristics by the ring oscillator, which can be used to emulate mechanoreceptors and artificial nerve fibers. The electrical signal from the artificial nerve fiber can be converted into PSC via a synaptic transistor. The decoupling and analyzing of signals from multiple mechanical stimulations are also critical to realize spatiotemporal recognition on multiple stimulus signals (Fig. 6f). By analyzing the frequency information of electrical signals from multiple resistive mechanoreceptors, the demonstrated artificial afferents can be used to realize shape recognition, motion detection, and braille recognition in simple scenes [31].

Stretchable NTS based on elastic rubber materials is able to exhibit a full range of synaptic properties, which can even retain 50 % of the initial synaptic properties under the stretching state [99]. In the stretchable NTS, rubber-based resistive mechanoreceptor is used to detect external physical stimuli. The induced presynaptic pulses can excite synaptic transistors to generate PSC, which are demonstrated to be capable to activate the biological nerves or engineering counterparts. Even under the stretching state, the PSCs mapping can be obtained based on the sensory pixels in the NTS array.

A resistive NTS by integrating ultrasensitive pyramidal pressure sensor array for tactile sensing and a flexible memristor array for multi-sensory data processing is recently reported by Chen's group, which enables near-sensor analogue computing. The core of this resistive NTS array utilizes a memristor computing array that enables vector–matrix multiplication operations, allowing direct processing of multiple tactile signals captured by the pressure sensor array without the need for analog-to-digital conversion. Flexible memristor array based on a stacked dielectric

structure of Au/TiW/HfO₂/Au works as the key computation component, exhibiting reliable and reproducible switching behavior, multilevel and stable conductivity states, and good flexibility. The resistive NTS can detect pressure signals in real time and is expected to be mounted on a finger or prosthesis to detect edge information of external objects. Moreover, the response time for one time operation of the sensing-computing process is 400 nanoseconds, and the average power consumption is 1000 times lower than that of the conventional interface electronic systems. This ultra-fast and energy-efficient artificial skin system will reshape human–computer interaction in the future and change the operation fashion of many existing smart applications [100].

Piezoelectric neuromorphic tactile system

Applying pressures on specific materials with non-centrosymmetric structures (e.g., piezoelectric ceramics, wurtzite structures, and piezoelectric polymers) will induce piezoelectric potential [101–103]. The piezoelectric potential can be delivered to a synaptic device to construct a piezoelectric-NTS to perceive the spatio-temporal touch information (Fig. 6d). For example, a piezoelectric graphene artificial sensory synapse is demonstrated by combining a piezoelectric nanogenerator (PENG) and an electrolyte gated graphene transistor. It can be regarded as a sensory nervous system by including sensing, transmission, and processing units [29]. Upon mechanical deformation, the dipoles in the piezoelectric polymer are aligned in a uniform direction to induce a piezoelectric potential, which promotes the PENG component to work as a self-powered mechanoreceptor. Under the influence of piezoelectric potential, ions in the electrolyte dielectrics will migrate and redistribute to regulate the conductance of graphene channel and induce PSC response. The relationship between the piezoelectric polarization induced by mechanical stimulation and the transport characteristics of semiconductors endows the PSC with temporal and spatial information of external stimuli. The unique ionic response behaviors and strong ion/electron coupling phenomenon at the interface of graphene/ion-gel lay the foundation for biomimetic nerve and biochemical sensing applications.

Inspired by the working mechanism of biological reflex, an NTS based on the piezoelectric effect of wurtzite-structured gallium nitride (GaN) is proposed, which can adjust the output of synaptic devices by directly responding to mechanical stimuli [104]. It utilizes a simple cantilever structure to realize the pressure sensing, which greatly simplifies the complexity of the system. A piezoelectric potential can be induced when the cantilever beam subjected to an applied strain, which will cause the concentration of two-dimensional electron gas to change at the interface of the semiconductor heterostructures. In this way, the piezoelectric potential can regulate the electron transport in the synaptic transistor to simulate the biological reflection process. This work demonstrates the output of synaptic transistor can be directly and effectively adjusted through weak mechanical stimulation.

Triboelectric activated neuromorphic tactile system

Based on the contact-electrification effect, the mechanical displacement of the triboelectric nanogenerator (TENG) can gener-

ate triboelectric potential and provide energy for distributed electronic devices or sensors in the Internet of Things [105,106]. By coupling the triboelectric potential with a semiconductor device, the electronic transport characteristics of semiconductor channel can be directly and actively controlled by mechanical input [103,107,108]. The combination of TENG and synaptic device can directly link the mechanical actions with artificial synaptic behaviors, demonstrating a prototype for more realistic neuromorphic devices (Fig. 6e). Several triboelectric-NTSs have been reported, including tribotronic EGFET [109], tribotronic FeFET [110], tribotronic FGFET [66], and tribotronic SFGFET [70]. The external mechanical actions exerted on TENG can be easily converted into voltage spikes (i.e., action potentials), which can be captured by synaptic devices to identify the coded spatiotemporal input characteristics and transmit corresponding feedbacks (or regulating instructions). In addition, the converted mechanical energy can be used to drive the synaptic device in a self-powered way, which can significantly reduce energy dissipation.

Based on the working mechanism of triboelectric-NTS, an artificial afferent nerve activated by contact electrification has been proposed to simulate the function of human sensory system. The triboelectric-NTS is composed of a self-activating component (TENG) and a MoS₂-based EGFET. As the TENG mechanoreceptor can be designed to work in different modes, it can be used to monitor different types of stimulus information including mechanical displacement, lateral-sliding motion, tactile signal, and pressure. The triboelectric signals activated EGFET further endows the system with the ability of spatiotemporal recognition on external stimuli. The demonstrated artificial afferent can be used to build dynamic logic and identify the frequency/amplitude of external actions. Recognition on spatiotemporal touch patterns has also been successfully proved to trigger corresponding LED logic (simulate the behavior of a virtual stimulus in the cerebral cortex) [32].

A triboelectric-NTS based on tribotronic FeFET is also constructed by coupling triboelectric effect with soft organic FeFET [110]. Triboelectric potential by mechanical stimulation induces the dipole alignment in ferroelectric gate dielectrics to modulate the PSC signals. In the tribotronic FeFET, tunable synaptic weights can be achieved by changing the composition of ferroelectric layer. The number and sequence of external touches can also be recognized through the triboelectric-NTS without additional signal processing circuits.

A versatile mechanoplastic triboelectric-NTS is also achieved based on tribotronic FGFET, in which the terminology of “mechanoplastic” is named relying on the utilization of mechanical behavior to regulate synaptic plasticity [66]. The mechanoplastic triboelectric-NTS is composed of a TENG artificial mechanoreceptor and a MoS₂ synaptic transistor with floating gate. The mechanical displacement can induce triboelectric potential to couple with the FGFET, trigger PSC signal, adjust synaptic weight, and realize the mechanical behavior-derived synaptic plasticity (i.e., mechanoplasticity). Thanks to the charge trapping in floating gate, the system can implement both STP and LTP controlled by mechanical displacement in an active and interactive way. Based on the LTP behaviors, neuromorphic logic switch (AND and OR) can be successfully implemented through the mechanoplasticity without complex CMOS circuits.

Under the synergistic effect of mechanical actions and semi-floating gates, a SFGFET based on graphene/hexagonal boron nitride (h-BN)/tungsten diselenide (WSe₂) vdW heterostructure has also been demonstrated with mechanoplasticity, including mechanical facilitation/depression, mechanical action derived STP/LTP, and learning behaviors [70].

EDL structure based neuromorphic tactile system

The EDL-NTS based on individual EDL structure allows the integration of perception, recognition, and transmission functions (Fig. 6g) [111]. The reported EDL-NTS consists of two conductive graphite electrodes drawn on a paper substrate, in which the two electrodes are opposite to each other and separated by a spacer. The EDL structure is equivalent to a device composed of multiple resistor units, which can be used for multi-point stimulation. The location of the mechanical stimulus can be determined by analyzing the magnitude of resistive response, thus mimicking the temporal and spatial dynamic logic function of biological neural network. The EDL-NTS has the advantages of fast response, good durability, personalized/custom tailing, and “zero” quiescent dissipation. In addition, the device is flexible and has the potential to be selectively drawn in arbitrary patterns, which is promising to achieve sophisticated paper-based neuromorphic tactile systems.

Artificial reflex arc

The transmission pathway from mechanoreceptor to synaptic device is the front-end of the whole neuromorphic tactile system. Synaptic devices can be used to connect with biological efferent nerves (or engineering counterparts) to form the complete artificial or (hybridized) synaptic reflex arcs (Fig. 6h) [31]. For example, the NTS can be connected to a motor/control unit (e.g., insect leg [31], actuator [112,113], pneumatic robot [99]) to construct a hybrid bioelectronic reflex arc to simulate the activation process of muscles. These systems have shown huge potentials in the applications of neurorobotics and neural prosthetics.

In addition to emulating the basic reflex arc by resistive-NTS [31], more adaptive functions can also be achieved through triboelectric-NTS/piezoelectric-NTS. Based on a triboelectric-NTS and a soft pneumatic robot with functional elastic skin, the soft robot uses artificial synapses to store encoded signals to programmatically sense mechanical taps for adaptive motions [99,104]. Inspired by reflex arcs, a piezoelectric-NTS-based strain-controlled power device can quickly and directly adjust the output response to external strain, which can be used to directly control the output signals by acceleration (or implement recognition on acceleration feedback). The piezoelectric-NTS can also be used to simulate the automatic adjustment functions based on the output signals in intelligent devices, exhibiting great potential for emergency braking in automatic driving or posture adjustment in robots. The demonstrated acceleration feedback control system proves the feasibility of NTS to providing appropriate feedbacks to external mechanical stimuli, which can help to enrich more advanced applications of bioinspired interactive neuromorphic devices [104].

Although various NTSs have been proposed and well developed, there are still some problems to be solved. First, the device structure is relatively monotonous. Synaptic transistors based on

sensory stimulation are still dominant, which limits the development of NTS toward multifunctionality. In the future, it is necessary to develop other alternative devices or configurations for sensory and neuromorphic components, which is of great significance to enrich more functionalities of NTS. Second, the use of ionic dielectrics reduces the power consumption of the device, but it introduces environmental instability against temperature and humidity. Therefore, appropriate encapsulation of the device needs to be considered. Third, the complexity of the device array inevitably increases with the increased number of sensory units. Therefore, constructing highly integrated array without increasing the complexity is an important task for NTS applications. Although the integration level of the demonstrated NTSs is still far below the biologically counterparts, it is highly required to take the first step toward high-density and robust interactive neuromorphic devices.

Bioinspired neuromorphic visual system

Human retina is composed of countless and intricately arranged photoreceptor cells and protrusions, which are connected to the visual center of the brain through nerve fibers to form the human vision system (Fig. 7a) [9,114]. The essential feature of retina-inspired neuromorphic visual device is that the synaptic weight (conductivity) can vary or even be preserved in response to the incident light signal [115–118]. Early strategy to realizing visual perception is commonly relying on the simple integration of photodetector and nonvolatile memory [27,112]. In recent years, machine vision technology has been rapidly developed for autonomous vehicles and robots. In principle, images (composed of pixels) are first captured by cameras with active pixel sensors, then converted from optical to digital format, and finally processed using machine learning algorithms (e.g., ANN, deep convolutional neural network (CNN), and reinforcement learning algorithms). However, this technology has encountered several intractable problems during its development: (i) images captured by camera generate a large amount of redundant data; (ii) there are efficiency bottlenecks in converting data from optical to electrical domain; (iii) data exchange between sensing and processing units results in latency power consumption; and (iv) complex images require incompatible pre-processing. Hence, simulating the neurobiological structure and the function of retina, developing photodetectors with memory functions, and attempting to directly modulate synaptic weights with light signals are expected to help solve these problems and provide a promising approach to visual sensing [11]. Such synaptic devices are usually required to have a persistent photoconductive (PPC) effect [119], i.e., where the conductance can be maintained for a long time after removing the light stimulus. Two main strategies based on the PPC effect have been proposed for neuromorphic visual devices. One approach is to directly utilize the intrinsic photosensitive memory properties of the material itself, and the other approach is to use a stacking strategy to indirectly confine photogenerated electrons/holes through heterostructure formed by stacking wide/narrow bandgap materials [119,120]. Inspired by human vision system, the neuromorphic visual systems based on low-dimensional materials (0D [40,121], 1D [9,122–125], 2D [126–128], and heterostructures

[12,129]), inorganic bulk materials (amorphous oxide semiconductor [7,8,130], molybdenum oxide (MoOx) [131], etc.), and organic semiconductors [132] have been intensively investigated (Fig. 7b, Table 2). For neuromorphic computing, recognition accuracy and efficiency are highly dependent on the linearity/symmetry of weight-updating curves and the number of effective conductance states [133]. Fig. 7c depicts the weight-updating mechanism for ANN simulation based on potentiation/depression (P/D) curves. The device conductance is in function of the pulse number (both positive and negative stimuli pulses). In the ideal case (dashed line in Fig. 7c), the conductance increases linearly with positive pulses and decreases linearly with negative pulses. However, most synaptic devices commonly exhibit asymmetric and nonlinear behaviors (where the conductance changes sharply and reaches a saturation state) [33]. Simulations are usually performed based on a two-layer ANN using standard gradient descent techniques (e.g., the backpropagation algorithm, Fig. 7d). Based on the photosensitive properties of the above materials (or structures), it is facile to utilize the photoconductive effects to simulate the function of photonic synapses, which have shown great potentials in image sensing and processing [131], visual assisted learning, color recognition, photoelectric logic operation, and bionic optoelectronic somatosensory systems (Fig. 7f) [12,112,128,131,134,135].

Low-dimensional materials/structures for neuromorphic visual system

0D materials

0D materials are a class of nanomaterials with internal electron motion confined in all directions, exhibiting many unique physical and chemical properties due to the significant quantum confinement effect. The optical characteristics of 0D materials are suitable for implementing neuromorphic visual system [136]. Related photonic devices enable fast-response parallel communication and hyper-connectivity due to the transmission of photons without the spatial and power density limitations caused by wiring in electronic circuits. Among various 0D materials, perovskite quantum dots (QDs) have narrow exciton binding energy, excellent absorption properties, and long charge carrier lifetime, which makes them (and related heterostructures) as potential candidates for excellent photosensitive materials. A photonic flash memory based on all-inorganic CsPbBr₃ perovskite QDs is fabricated to simulate synaptic functions [40]. The heterostructure formed between the CsPbBr₃ QDs and the semiconductor layer is the basis for the optically programmable and electrically erasable characteristics of the memory device. This mechanism can be used to simulate typical synaptic functions of STP, LTP, and STDP at the device level. Based on the photonic enhancement and electrical habituation, the synaptic weight exhibits multi-wavelength responsive characteristics. These results have laid the foundation for future developments of perovskite-type memories and synaptic devices with diversified plasticization means and sophisticated computation capacities.

Silicon nanocrystals are also widely used to fabricate synaptic devices, which enable the synaptic responses to light stimuli over a wide spectral range from ultraviolet to near-infrared [121]. The available synaptic plasticity of silicon nanocrystal-based synaptic

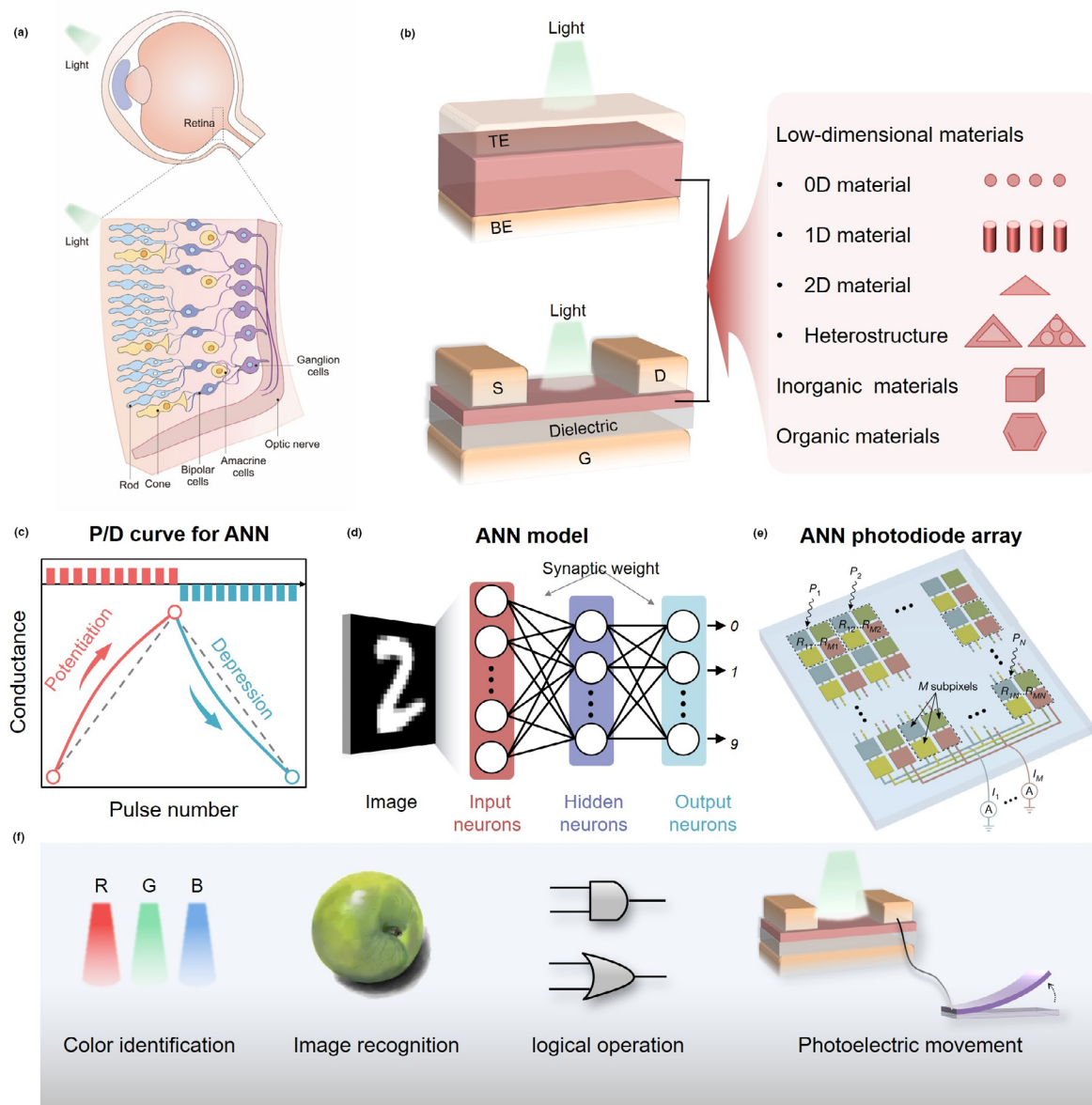


FIGURE 7

Bioinspired neuromorphic visual system. (a) Schematic diagram of biological vision system. (b) Schematic diagram of neuromorphic visual system. (c) Potentiation/depression (P/D) curve for ANN simulation. (d) A two-layer ANN model for supervised learning. (e) An ANN photodiode array for sensing and processing optical images. (f) Applications of neuromorphic visual system.

devices is attributed to the dynamic capture/release of photogenerated carriers at the defect sites, e.g., dangling bonds on the nanocrystal surface. Intensive research on silicon nanocrystals in low-energy broadband photonic synaptic devices are of great significance to the large-scale deployment of conventional silicon materials in the emerging neuromorphic computing.

1D materials

1D material is a type of nanomaterial in which electrons are free to move in only one nanoscale direction. One of the most widely studied 1D materials is carbon nanotubes (CNTs), which are formed by convolving graphene sheet layers with metallic (or semiconducting) behaviors depending on its chiral vector. It has high charge carrier mobility with excellent physical and chemical stability, and is widely used as the channel materials

for three-terminal transistors [137–139]. Floating-gate synaptic transistors based on semiconducting CNTs can provide adjustable weight-updating linearity and variation margin, representing great potential to enable pattern recognition from the device-to-system level [10]. Meanwhile, combining CNTs with photosensitive semiconductor materials can be readily used to simulate optical synaptic behaviors. For example, Zhu et al. report a 1024-pixel flexible photosensor array based on CNTs/perovskite QDs as the active materials, in which a built-in electric field is formed at the interface to equilibrate the Fermi levels and plays a key role in the separation of photogenerated carriers. The demonstrated photosensitive device exhibits ultra-sensitivity and ultrahigh specific detectability for visible light. It can also directly respond to optical stimuli and perform optically tunable synaptic plasticity for preprocessing of visual information,

TABLE 2

Summary of bioinspired neuromorphic visual system (NVS).

AVS structure	Material property	Photosensitive material	Device structure	Stimulus signals	Synaptic behavior	Applications	Refs.
0D material-NVS	Narrow exciton binding energy; Excellent absorption properties; Long charge carrier lifetime	CsPbBr ₃ QD	FGFET	Electro-optical	STP/LTP, PPF/D, SRDP	-	[40]
		Cs ₂ AgBiBr ₆ QD	FGFET	Pressure-optical	PPF, LTP/D	Multisensory integration	[171]
		Si Nanocrystal	2-terminal	Optical	STP to LTP/STDP	-	[121]
1D material-NVS	Ultrahigh surface-to-volume ratio; Mechanical flexibility; Process scalability; Device miniaturization	CNT/CsPbBr ₃ QD	FET	Optical	PPF, STP to LTP	Reinforcement learning	[122]
		TiO ₂ nanowire	Memristor	Optical	STDP	-	[123]
		ZnO nanorod	Memristor	Optical	EPSC, PPF, STP	-	[124]
		ZnO nanowire	FGFET	Optical	E/IPSP, PPF, STDP	Pattern recognition	[186]
		InGaO ₃ (ZnO) ₃ superlattice nanowire	FET	Optical	PPF, STDP	Orientation selectivity, image memorizing	[125]
2D material-NVS	Compatible with planar wafer technology; Excellent electrostatic tunability; Large on/off ratios for TMDC; Ultrathin body and unique band structures; High thermal stability; Controllability of the synaptic weights Unique optical characteristics; Broad spectral range	W/MoS ₂ /p-Si	Memristor	Electro-optical	E/IPSP, STP to LTP	Photonic potentiation, electric habituation	[126]
		MoS ₂	EGFET	Electro-optical	LTP/D, STDP	Pavlovian conditioning	[127]
		WSe ₂	Photodiode array	Optical	-	Image recognition and encoding	[11]
		ReS ₂	Memristor	Optical	EPSC, PPF, LTP	Training, recognition and inference	[119]
		MoSSe	FGFET	Electro-optical	PPF, STP, LTP/D, SNDP	Image pre-processing and recognition	[187]
		BP	-	Optical	E/IPSC, PPF, STDP	Optical logic operation	[128]
Heterostructure-NVS	Stackable and designable; Heterogeneous integration; Expandable to other materials; Excellent optoelectronic performance; PPC effect	Graphene/CNT	FET	Optical	STP/LTP	Optical logic operation	[157]
		CsPbBr ₃ QD/MoS ₂	EGFET	Electro-optical	PPF, STM/LTM	Conditioning, neural coding	[188]
		WSe ₂ /h-BN/Al ₂ O ₃	FET	Optical	-	Image sensing and processing.	[129,189]
		BP/Al ₂ O ₃ /WSe ₂ /h-BN	FET	Optical	-	Motion detection and recognition	[190]
		h-BN/WSe ₂	FET	Optical	LTP/LTD, STDP	Color recognition	[12]
		MoS ₂ /pV3D3	Phototransistor	Electro-optical	STP/LTP	Image acquisition, pre-processing	[191]
		Graphdiyne/graphene	Transistor	Electro-optical	E/IPSC, LTP/D	Logic operation, image distinction	[192]
		MoSe ₂ /Bi ₂ Se ₃	RRAM	Electro-optical	STP, LTP, PPF/D	Visual information storage	[43]
		Graphene/MoS ₂	FET	Tactile-optical	LTD	Image recognition	[13]
Oxide-NVS	High mobility; Large bandgap; Optical transparency; Low temperature synthesis; Excellent large-area uniformity; Adjustable composition	IGZO-alkylated GO	FET	Electro-optical	LTP/D	Image recognition	[8]
		IZO, ISZO, ISO, IZO	FET	Optical	S/LTP, STDP, PPF	-	[7]
		SnO ₂	FET	Electro-optical	PPF/pain perception	Optical logic operation	[193]
		ITO/In-TiO ₂ /Au	Memristor	Optical	EPSP/IPSP	Sensorimotor	[135]
		ITO/MoOx/Pd	RRAM	Optical	STP to LTP	Image recognition	[131]
		ITO/HfOx/TiN	Memristor	Electro-	LTP/D	Image filter	[194]

(continued on next page)

TABLE 2 (CONTINUED)

AVS structure	Material property	Photosensitive material	Device structure	Stimulus signals	Synaptic behavior	Applications	Refs.
		ZnO/ATO/FTO	Memristor	optical		Photonic nociceptor Motion/handwritten detection	[130]
		ITO/ZnO/Nb-STO	Photomemristor	Optical Pressure- optical	-		[195]
PCM-NVS	Non-volatile, reproducibility and stability	Ge ₂ Sb ₂ Te ₅ /Si ₃ N ₄	Photonic memory	Optical	-	Optical logic operation	[134]
Organic-NVS	Flexible; Low Cost; adaptable by chemical design; Compatible with large- area printing methods	Organic molecular	Phototransistor	Optical	STP/LTP, STDTP	Visual perception	[132]
		IDTBT: PCBM	Phototransistor	Electro- optical	E/IPSC, PPF/D, S/ LTP	Image recognition	[196]
		PTCDI-C8/VOPc	FeFET	Optical	STP/LTP	Color recognition	[27]

exhibiting great potential as a neuromorphic visual system. All the demonstrations provide impetus for the development of simulated neuromorphic visual systems to mimic the flexibility, complexity, and adaptability of biological visual systems [122].

Semiconductor nanowires/nanorods constitute another large category of 1D materials [136]. Nanowires with fine morphology and uniform diameter are usually grown via a bottom-up vapor-liquid-solid (VLS) method. The prepared nanowires can be transferred to any substrate (e.g., flexible substrates) by a mature process with good compatibility between the target substrate and the nanowire growth process [125]. In addition, nanowires/nanorods have excellent photoresponsive properties superior to conventional photonic materials because of the ultra-high surface-to-volume ratio of the 1D morphology [140]. A series of semiconductor nanowires/nanorods (e.g., TiO₂ nanowires [123], ZnO nanorods/nanowires [124], InGaO₃(ZnO)₃ superlattice nanowires [125]) has been successfully used in neuromorphic visual devices. The demonstrated enhancement of learning behaviors depends on the temporal correlation and the number of light pulse stimuli, which is consistent with the spike-time-dependent plasticity. The working mechanism can be attributed to the adsorption-dissociation kinetic behaviors of oxygen molecules on the nanowire surface, similar with the Ca²⁺ flow and neurotransmitter release kinetics in biological synapses. To achieve a more realistic visual system, Gu et al. construct a spherical bionic electrochemical eye (EC-EYE) with a larger viewing angle compared to planar-type optic [9]. Perovskite nanowires are used to mimic human eye's optic rod cells, and high-density nanowire arrays grown via a vapor-phase approach are assembled in a hemispherical porous transparent insulating template to mimic the human retina. The ionic liquid electrolyte is used as the front contact of the nanowire, while the liquid metal wires are used as the back contact of the nanowire photosensors, mimicking the human nerve fibers behind the retina. EC-EYE has exhibited high responsiveness, reasonable response rate, low detection limit, and wide field of view. In addition to being structurally similar to the human eye, the nanowires used in the hemispherical artificial retina have much higher density

than the photoreceptors of the human retina, allowing higher imaging resolution by implementing a proper contact strategy.

2D materials

2D materials with the unique 2D structure exhibit many surprising and peculiar properties because the motion of free electrons in 2D materials is only in two dimensions. Compared to 0D and 1D materials, 2D materials offer better device scaling and integration with existing planar wafer technologies [136]. Following the discovery of graphene in 2004, other 2D materials (particularly TMDs) have become the hotspot in scientific research [141]. Each layer in 2D materials is connected by covalent bonds, with no dangling bonds on the surface and weak vdW forces between the neighboring layers [142]. Benefiting from this unique layer structure, electrons can be confined in the ultrathin body of the 2D semiconductor and precisely tuned by the electric field [143]. Single layer or few layers 2D materials can be easily exfoliated off from the bulk 2D crystal. However, the shape, size, and thickness of the 2D material flakes obtained via top-down mechanical exfoliation approach are non-uniform, which makes the further scaling at macroscopic scale remain a challenge [144]. Recently, using improved exfoliation process through interfacial interactions, e.g., gold-assisted exfoliation [145], is expected to overcome this challenge. In contrast, the bottom-up chemical vapor deposition approach is more advantageous in growing monolayers 2D materials [146]. Among the family of 2D materials, graphene has the advantage of high carrier mobility but poor photosensitivity; TMDCs (e.g., MoS₂, WSe₂, ReS₂) have strong visible light absorption due to their wide band gap. BP has a high hole mobility ($\approx 10^3$ cm² V⁻¹ s⁻¹), highly anisotropy, a thickness-tunable band gap ranging from 0.3 to 2 eV, strong light-matter coupling, and a wide spectral range from deep ultraviolet to infrared waves, but poor air stability [147–150]. Monolayer MoS₂ is a direct bandgap semiconductor with high absorption coefficients and efficient electron-hole pair generation under light excitation, which is highly suitable for applications in optoelectronic devices due to the quantum mechanical constraints [151]. On this basis, a photon-

enhanced memristive device based on a monolayer MoS₂ is successfully fabricated [126]. Basic characteristics of photonic synapse are demonstrated based on the inherent persistent photoconductivity and volatile resistive switching behavior of MoS₂ [126,127]. Based on the inherent light-sensitive memory properties of ReS₂, it is able to modulate the synaptic weights via light stimuli, thus mimicking the dynamics of biological synapses, e.g., excitatory post-synaptic current (EPSC), PPF, and LTP [119]. BP-based three-terminal optical synaptic devices have also been used to simulate the process of learning and forgetting behaviors, also exhibiting excellent performance in optoelectronic logic operations [128]. The bioinspired vision sensors based on MoS₂ phototransistors can achieve dynamic modulation of the photosensitivity under different illumination conditions, which can be used to emulate adaptive artificial retina. This MoS₂ phototransistor array exhibits both scotopic and photopic adaptation, providing a wide perceptual range and enhanced image contrast [14]. Another image sensor array based on WSe₂ photodiodes has also been demonstrated by building an ANN for sensing and processing the images projected on the photonic sensory array. The photosensitivity of each photodiode can be readily tuned by the gate voltage, which is critical to realize modulation on connection weight in ANN and implementation of simple computational tasks (Fig. 7e) [11].

Heterostructures

Among the active materials for photonic synapses, binary or heterostructures constructed by 2D materials [73,74,152–155] offer distinctive advantages of high photocurrent, excellent quantum efficiency, and ultra-fast photoresponse. Van der Waals heterostructures with defect-free interfaces [156] can maintain high electron mobility and exhibit typical photoresponsive characteristics according to the gate tunable charge transfer/exchange between layers. For example, STP behavior can be achieved by charge transfer between graphene and SWCNT heterostructure, which is not observed in pure CNT devices [157]. Moreover, due to the presence of charge traps between the heterostructure and the substrate interfaces, the heterostructure synapses are non-volatile with gate-controlled PPC effects, exhibiting a well-mimicked LTP behaviour [157]. Based on the gate tunable photoresponse of BN/WSe₂ heterostructures, the neurobiological functions of retinal cells have been successfully emulated [12,129]. Based on a neuromorphic visual system constructed in a matrix array, simultaneous image recognition and processing can be realized by the reconfigurable vision sensor by adjusting the gate voltage applied on each pixel. The demonstrated vision sensor offers a reliable prototype to endow visual neural networks with convolutional computation capabilities [129]. After an in-depth study of the synaptic behaviors by means of machine learning, an artificial visual neural network based on the BN/WSe₂ vdW heterostructure is also constructed to simulate the color recognition function of human visual system (similar to the color blindness test) [12]. Optoelectronic synaptic devices that combine photons and electrons have promising applications in interactive neuromorphic devices to mimic the retina. However, existing neuromorphic visual systems are limited by the requirement of electrical stimulation to implement bidirectional synaptic weight updating. Hou et al.

report a flexible wafer-scale two-terminal all-optical modulated synaptic device. Based on pyrenyl graphdiyne (Pyr-GDY)/graphene/PbS quantum dots heterostructures, the device can simulate both excitatory and inhibitory synaptic behaviors in optical circuits. Additionally, the device has exhibited a series of logical functions and associative learning capabilities, which may significantly enhance the information processing capabilities of neuromorphic visual system [133]. Recently, Pi et al. demonstrates the possibility of band alignment between type-II and type-III heterostructures (e.g., palladium diselenide (PdSe₂)/MoS₂ heterostructures) for neuromorphic vision applications. The type-II and type-III heterostructures have a gate-tunable positive and negative photoresponse, as well as a broadband linear gate-dependence photoresponsivity, which allows different types of convolutional processing for remote image sensing. Compared with conventional single-band-based convolutional neural networks, this device is able to provide both broadband image sensing and convolutional processing to improve the recognition accuracy of multi-band images [158].

Inorganic materials/structures for neuromorphic visual system

It has become a major research direction to seeking efficient materials suitable for photonic neuromorphic devices to simulate the behavior of photo-synapses and construct interactive neuromorphic visual systems. Based on the inherent PPC of some materials, the function of photonic synapses can be successfully emulated. Amorphous oxide semiconductors, represented by indium-gallium-zinc oxide (IGZO) [8] and indium-zinc oxide (IZO) [7], have the advantages of high mobility, large bandgap, good optical transparency, and excellent large-area uniformity. The effects of ionized oxygen vacancies on the generation/relaxation of photogenerated carriers can be used to emulate the typical behaviors of photonic synapses (e.g., STP/LTP, time-dependent plasticity, and PPF). Two-terminal synaptic device based on Pd/MoO_x/ITO (ITO is indium tin oxide) has been fabricated for ultraviolet sensing and demonstrated as light-triggered nonvolatile switch and light-tunable artificial synapse [131]. Relying on the stable switching between high and low resistance states, the prepared photonic synaptic array can further implement the functions of image recognition/memory and neuromorphic visual preprocessing, which significantly helps to improve the processing efficiency and image recognition rate for postprocessing tasks.

Organic materials/structures for neuromorphic visual system

Organic materials are flexible, adaptable by chemical design [48,54], and compatible with large-area printing methods [31,96]. In OFET, the interface effect (between the semiconductor channel and dielectrics) has significant influences on device photosensitive properties, which can be used to simulate the behaviors of photonic synapses [132,159]. In particular, OFETs have shown signal additive properties caused by repetitive light pulses, which are suitable for light-stimulated artificial synapses. However, the high operating voltage of conventional OFETs results in high energy consumption and hinders their further applications in neuromorphic visual system. To solve this problem, Shi et al. report an all-solution-printed OFET array for neuromorphic visual system with ultra-low energy consumption of

0.07–34 fJ per spike. By introducing a Schottky barrier at the source-semiconductor contact, the charge carrier injection can be readily tuned to allow the OFET to operate under a low driving voltage, thereby reducing its power dissipation. Furthermore, an artificial visual neural network based on the 8×8 OFET arrays has also been demonstrated on a flexible substrate, exhibiting excellent performances on low-power-consuming image recognition/enhancement. This work has opened up the path toward ultralow-energy-consuming organic neuromorphic visual systems [160].

Light stimulation of synaptic devices is critical to the development of neuromorphic computing with wide bandwidth and high-efficiency communications. Various modes of light signals can activate the photodetector to generate voltage pulses, which are generally applied as the presynaptic spikes to trigger EPSC in the synaptic devices. Corresponding postsynaptic responses can be used to simulate the function of human eyes for visual aided learning and color recognition [12]. The synaptic responses containing spatio-temporal information can also be delivered to target effectors (the reflection of the muscle [112] or the light interactive actuator [135]). For example, a photo-interactive artificial neuromuscular system is constructed to simulate the neuromuscular function, which utilizes optoelectronic organic synapses as the photodetector and stretchable organic nanowires as the actuator. The voltage pulses produced from the self-powered photodetectors (triggered by light signals) can be used to drive the integrated organic synaptic transistors. After cognitive processing, the obtained synaptic output information can be used for human-machine interaction. Besides, optical wireless communication of the interface can be used for optical actuation of artificial muscles. In another typical example, optical inorganic synapses (indium-doped TiO_2 nano-film) are activated to stimulate the liquid-metal-based actuators [135]. The optoelectronic synapses can produce excitatory and inhibitory postsynaptic signals to trigger the vibration behaviors of liquid metal droplets, thus simulating the expansion and contraction of biological muscle fibers. This new artificial optoelectronic sensory system is highly promising for potential light-excitation response in biological motion systems.

Bioinspired neuromorphic auditory system

As an auditory organ, the ear perceives and distinguishes the characteristics of sound when it receives sound waves (Fig. 8a). The brain can help to analyze the location of sound by interaural time difference (ITD, Fig. 8b). ITD refers to the time difference when the sound wave reaches the left and right ear due to the distance between the two ears, which is the most important clue of sound location. Based on the capacity of precise spike timing, a spatiotemporal neural network based on resistive switching neuromorphic auditory system (NAS) is constructed to mimic the function of sound azimuth detection by human brain [161]. By detecting the ITD with suppressed synaptic-weight dependence on sound amplitude/frequency, the sound localization can be realized based on a designed circuit with excitatory/inhibitory-adjustable synaptic devices (Fig. 8c) [162]. Assisted with resistive channel and capacitive gate, an artificial time-delay neuron based on MoS_2 FET is fabricated to simulate

a limited axonal conduction velocity, which is very important for translating the ITDs into a spatial computational map [163]. A hybrid synaptic transistor based on WSe_2 and MoS_2 vdW heterostructure is also designed to selectively potentiate and depress the channel conductance for acoustic pattern recognition assisted with ANN simulation (Fig. 8d) [164]. The above results show that based on the excitatory/inhibitory characteristics of NAS and combined with suitable neural circuits or algorithms followed by recognition, it is possible to achieve real-time speech biometrics, sound localization, and precise synaptic information processing functions [161–167].

Bioinspired neuromorphic multisensory system

In order to achieve sophisticated and precise operations, robots are usually equipped with a variety of sensors. Usually, different types of sensors sense external signals independently and convert them into electrical signals, which are further encoded and transmitted. This approach generally enables the processing of asynchronous temporal information, but has difficulty in handling more complex information, which severely degrades the intelligence of the system [168]. Therefore, parallel processing of sensory signals is of crucial importance in the novel computing paradigm. It remains a challenge to perform real-time parallel processing of external sensory information transmitted by multiple sensory neurons and respond independently to the integrated sensing information through artificial efferent nerves [169]. The following strategies can be implemented to integrate different neuromorphic devices into a single system. One typical strategy is data fusion, e.g., visual-tactile fusion [13,170,171], tactile-olfactory fusion [172], and multisensory fusion [5]. Joint sparse coding and deep learning provide effective methods for multimodal fusion and feature extraction [173]. Pre-processing different data with the help of algorithms and other means can solve the problems of data type, dimensionality, and sparsity mismatch [170]. Multimodal fusion strategies have been shown to improve the recognition accuracy and have potential applications in disaster response [172]. However, this approach is limited by the size of the sensor to be further integrated, which is too bulky and rigid to form intimate contact with the user for high-quality data acquisition [170]. Another approach is to use the intrinsic properties of functional materials, such as piezoelectric properties, optoelectronic properties, temperature and humidity sensing properties, chemical sensing properties, etc. 2D materials are one of the promising materials (especially in optoelectronic properties with high sensitivity and good reliability), allowing to maintain the high quality of sensing signals and simplify the complexity of system integration [13].

Bioinspired neuromorphic tactile-visual system

Associate analysis of biological mechanical motions and visual information is a fundamental perceptual and cognitive ability of human brain, which is of great significance in acquiring somatosensory and visual data to simulate artificial intelligence (Fig. 9a) [152,170]. Therefore, it is very important to achieve multimodal plasticity of interactive neuromorphic devices by updating synaptic weights through the mechanical-optical synergistic effect.

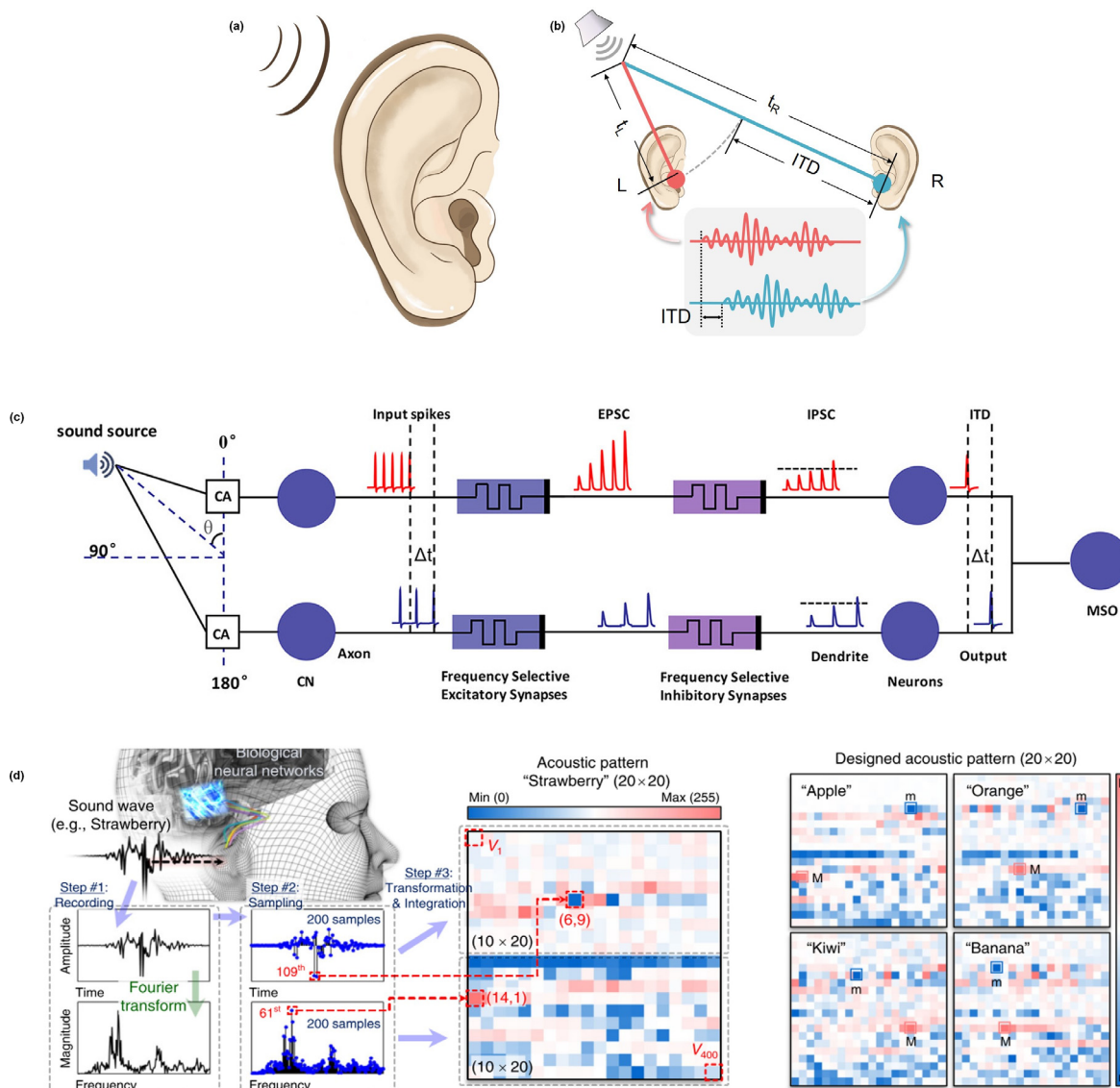


FIGURE 8

Bioinspired neuromorphic auditory system. (a) Biological auditory system. (b) Schematic diagram of interaural time difference (ITD). (c) Working mechanism of synaptic computation for ITD-based sound localization. (d) Acoustic pattern recognition by hybrid synaptic transistor based on vdW heterostructures.

As is known, over-reliance on vision can be problematic. In dynamic environments, factors such as optical occlusion and dark scenes often severely affect the accuracy of image recognition [170,172]. In the absence of continuous line-of-sight, only vision information may make it difficult to achieve manual dexterity in robotic operations, e.g., searching for wreckage in disaster response [93]. To improve recognition accuracy, visual data can be combined with other types of information data captured from different sensors for data fusion [168,173]. For instance, the tactile mode is used for local information and the vision mode is to provide the global picture [173]. The earliest attempts to fuse vision and tactile to recognize/represent objects can be dated back to the 1980s [174]. Tactile sensing aiding visual sensors is able to extract more features to improve the performance of object recognition [175], object reconstruction [176], and grasping [177,178], providing local and detailed information [179] to deliver related knowledge with vision [173].

Visual and tactile modes are different in format, frequency, and information range. In addition, certain features can only be acquired through a single sensory mode. For example, the color of an object can only be obtained visually, while the texture, hardness, and temperature of a surface can be obtained through tactile sensing. Asynchronous information obtained from two modes and different sensing ranges poses a great challenge for multimodal fusion [168]. Chen's group has developed an artificial sensory neuron with visual-haptic fusion [180], where photodetectors and pressure sensors can convert external tactile and visual stimuli into electrical signals, respectively. The electrical signals from these two sensors are then transmitted via ionic cables to synaptic transistors for integration and conversion into EPSC. Based on the PPF effect, successive stimuli cause an increase in EPSC spikes, which can be used to determine the degree of synchronization between the two spikes. Conducting this process in turn can help to provide multidimensional spatial

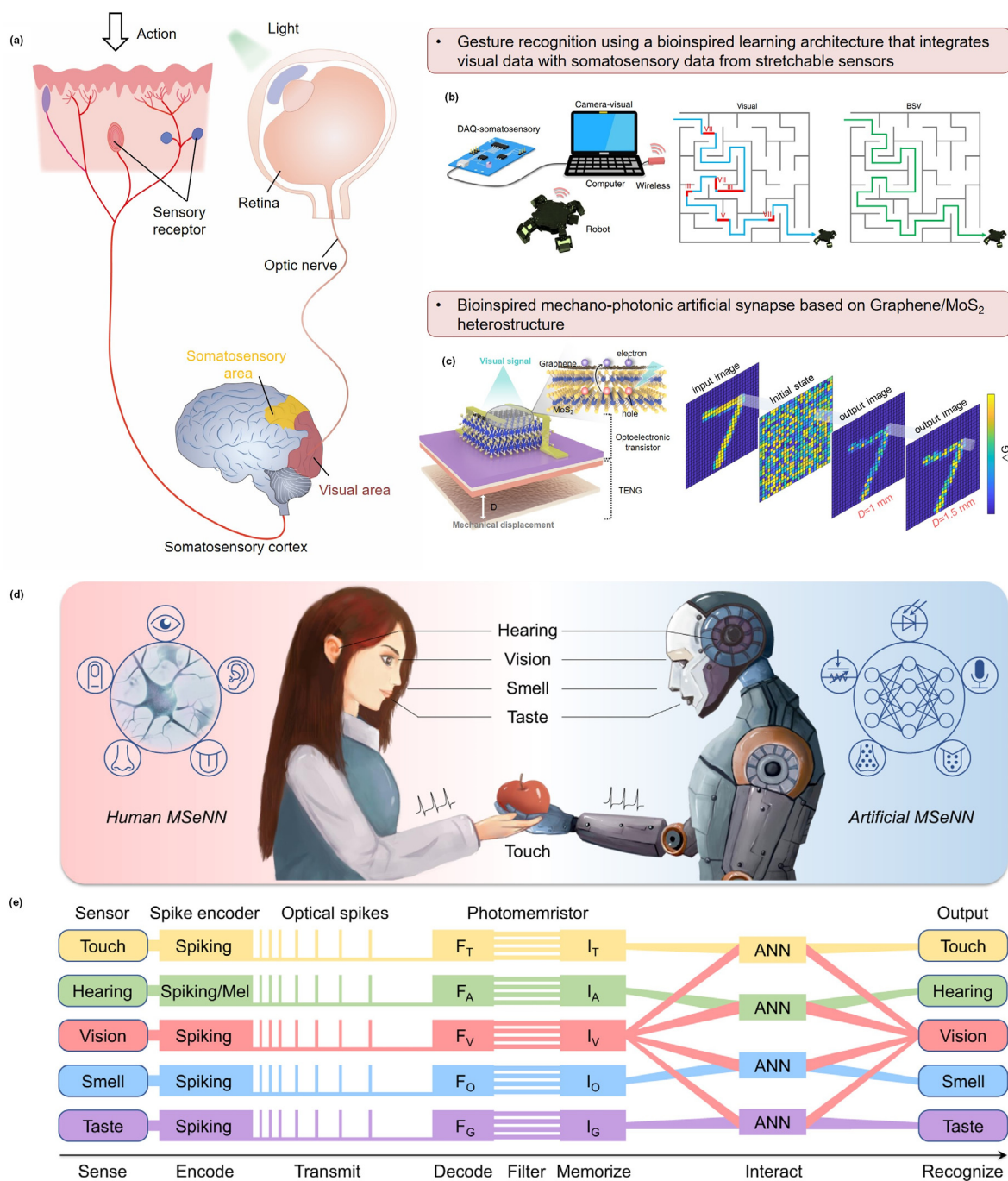


FIGURE 9

Bioinspired neuromorphic multisensory system. (a) Biological tactile-visual system. (b) Bioinspired data fusion architecture. (c) Bioinspired mechano-phonic artificial synapse. Schematic of (d) the human and (e) artificial multisensory neural network.

information to control neuromuscular junction or a robotic hand for action perception, processing, and feedback. This group has also developed a bioinspired data fusion architecture (Fig. 9b) [170], which can realize gesture recognition by integrating visual data and somatosensory data (obtained from a stretchable strain sensor based on single-walled CNTs). The architecture uses convolution neural network for visual information processing, and then uses sparse neural network at the feature layer for fusion and recognition of somatosensory data. The fusion architecture

maintains recognition accuracy under non-ideal conditions of noisy and under-/over-exposed images.

Another strategy to neuromorphic tactile-visual system is to embody the intrinsic photosensitive properties of the material to reduce the integration of the system. As mentioned above, the vdW heterostructures formed by stacking different 2D materials have rich electronic and optoelectronic properties [142]. These properties can be used to simulate the function of retinal neurons or construct a neuromorphic visual system based on

the intrinsic photosensitive properties. By combining graphene and MoS₂, the heterostructure with excellent optical sensing properties can be constructed. Such heterostructures with high photoelectric detection sensitivity and continuous gate-adjustable photoconductivity are prerequisites for the integration with artificial synapses in different modalities [73,74,155]. By combining triboelectric gating with photoconductive effects of photonic synapses, one can use an active and direct way to simulating the synaptic plasticity and multimodal neural functions. Sun's group [13] has introduced a bioinspired mechano-photonic artificial synapse with synergistic mechanical and optical plasticity, which consists of a graphene/MoS₂ heterostructure based phototransistor and an integrated TENG (Fig. 9c). A tunable photoresponse related to mechanical displacement is realized by controlling the charge transfer/exchange in the heterostructure with triboelectric potential. Based on the simulation of artificial neural network, it is proved that the image recognition rate is improved to 92 % assisted with mechanical plasticization. The artificial multisensory integration nervous system [171] based on the integration of a flexible TENG and a FGFET with Cs₂AgBiBr₆ QDs also coincides with this strategy. Based on this design, a 3 × 3 pixel array of artificial photosynaptic circuits driven by TENG is also developed and demonstrated with superiority of multisensory integration. Multisensory integration can effectively enhance the signal-to-noise ratio of images, improve image quality, and enhance the accuracy of pattern recognition, providing an efficient methodology in realizing mixed mode interactions, simulating complex biological neural systems, and facilitating the development of interactive artificial intelligence.

Bioinspired neuromorphic tactile-olfactory system

In addition to vision, the tactile and olfactory perception are other two key natural abilities that animals have evolved. Inspired by star-nosed moles, a star-nose-like tactile-olfactory sensing system is mounted on a robotic hand [172] to demonstrate tenacious object recognition in the presence of interference. The flexible sensing array on the robotic hand adopts silicon-based force and gas sensors with high sensitivity and stability to obtain reliable tactile and olfactory information by touching objects. With the help of machine learning, key features about the local topography, material stiffness, and odor of the tested object can be extracted. In this work, CNN and fully connected networks are used for early tactile and olfactory information processing, which resembles the function of the local receptive fields of the biological nervous system and mimics the initial processing of tactile and olfactory information in primary area (PA). Besides, fully connected networks can be used to extract features from the raw information and deliver pre-decisions on the output weights of tactile and olfactory information based on the surrounding environment, which realize the mimicking of signals interactions in the biological nervous system association area (AA). Based on the fully connected networks for multisensory fusion of tactile and olfactory information (similar with the biological information fusion process), the system can achieve the functions of object classification (96.9 % accuracy), human body recognition (>80 % accuracy) despite gas interference, object burial, damaged sensors, and hazardous situ-

ations of rescue missions. Compared to vision, the tactile-olfactory fusion strategy offers a possibility in dark or obstructed spaces and has a relatively small input data size, leading to smaller requirements for computational resources and faster recognition, which is crucial in rescue missions.

Other neuromorphic multisensory system

Since the world is multimodally interconnected, people learn and adapt to the ambient environment by sensing, interpreting, and most importantly, associating and learning from multimodal information from the environment. The integration and interaction of vision, touch, hearing, smell, and taste in human multisensory neural networks facilitates higher cognitive functions such as cross-modal integration, recognition, and imagery to accurately assess and fully understand the multimodal world. To make robots perceive more like humans, artificial multisensory systems with advanced cognitive sensing and multimodal environmental information processing functions are urgently needed. By integrating multisensory subsystems (including artificial vision, touch, hearing, smell, and taste sensors) and neural networks for multisensory data fusion, cross-modal learning can be readily achieved (Fig. 9d). In this process, distributed sensors are used to detect multimodal physical stimuli and convert the information into potential changes; spike encoders are used to encode potential changes into optical spikes; photomemristors are used to decode, filter, and memorize this information; and ANNs are used to correlate and learn the cross-modal signals. Ultimately, the perception, encoding, transmission, decoding, filtering, memory, and recognition functions of multimodal information are achieved, and it is also possible to fuse multisensory data at the hardware and software levels. Using cross-modal learning, the system is capable of cross-modal recognition and imaging the multimodal information, such as visualizing letters during handwritten input, recognizing multimodal visual/smell/taste information, or imaging never-before-seen pictures when hearing their description. Multisensory neural networks offer a promising approach to robotic sensing and perception [5].

Summary and perspectives

In summary, we have reviewed the recent progress on bioinspired interactive neuromorphic devices, classified as neuromorphic tactile systems, neuromorphic visual systems, neuromorphic auditory systems, and neuromorphic multisensory system. We discuss the interactive neuromorphic devices from the aspects of materials, device architectures, operating mechanisms, and potential applications. Multifunction-fused interactive neuromorphic devices are then proposed with promising multiple/mixed synaptic plasticity to address more realistic problems. In addition, we discuss the pros and cons regarding to the computing neurons and integrating sensory neurons (Table 3). The perspectives on bioinspired interactive neuromorphic devices are finally summarized at the material, device, network, and system levels. Computing neurons rely on centralized and sequential processing determined by clocks and perform high speed and accuracy for well-defined problems and repeated tasks [5,181]. Usually, external sensors are used to capture analog signals and convert them to digital format for

TABLE 3

The pros. and cons. about computing neurons and integrating sensory neurons.

Computing neurons	Integrating sensory neurons
<p><i>Pros.</i> Centralized and sequential processing [181] High speed and accuracy for well-defined problems [181] The external sensor captures the analog signal and converts it to digital format for processing using algorithms [182] Better integration with CMOS [183]</p>	<p>Distributed, parallel, and event-driven [181] Handle complex real-world problems (e.g., visual and speech recognition and motion control) [31] In-sensor computing with higher efficiency [3,31] Real-time sensing and processing with low latency [11] Optional connection to neural engineering counterparts for real-time sensing, processing and feedback [169] Simplify circuit and algorithm complexity [14]</p>
<p><i>Cons.</i> Time-consuming data conversion (e.g., optical image to electrical domain conversion) [131] Data redundancy, low efficiency, and high-power consumption [11] Complex circuits and algorithms [14]</p>	<p>Compatibility of sensors with synaptic devices Signal decoupling, signal interference High difficulty of on-chip integration</p>

processing using algorithms [182]. To implement this task, current systems use circuits and algorithms that compromise efficiency and increase complexity [14]. Data conversion is time-consuming and laborious (e.g., optical image to electrical domain conversion) and the data captured is large and redundant, which results in low computing efficiency and high-power consumption [131]. As these functions are implemented on the basis of silicon logic circuits, they are compatible with the existing infrastructure of silicon wafer technology [183]. In contrast, sensing units, neurons, and synapses in integrating sensory neurons process information based on distributed, parallel, and event-driven computation [181]. In-sensor computing with higher efficiency allows for the capture of large amount of data and performs low-latency real-time sensing and in-situ processing of the captured data, reducing the complexity of circuits and algorithms [3,11,14,31]. There is also the option to connect with neural engineering counterparts (e.g., artificial muscles, actuators, feedback devices) to realize the function of real-time sensing, processing, and feedback [169]. Through the combination of various sensors and synaptic devices, the bioinspired interactive neuromorphic devices provide solutions to next generation of sensing and computing different types of signals in large number. Neuromorphic tactile systems, neuromorphic visual systems, neuromorphic tactile-visual systems, and neuromorphic auditory systems have been successfully investigated in previous reports. However, research on interactive neuromorphic devices that utilize sensing and synaptic devices for perception and computation is just beginning and has a long way to go. Compatibility issues between sensors and synaptic devices, signal decoupling for multi-sensing coupling, interference, and on-chip integration need to be addressed urgently. Optimized sensors, neuromorphic devices, and hardware integrations with compatible algorithms are highly required. Fig. 10 shows a roadmap for the future development of bioinspired interactive neuromorphic devices, which is discussed from the prospects of interactive neuromorphic devices at the material, device, network, and system levels, respectively.

Materials

At the material level, there are mainly-two research directions. One is to explore growth conditions and modification processes

to improve the physical properties and interface quality of materials, and the other is to explore new materials with unique properties. Besides, the preparation of large-scale homogeneous novel nanomaterials remains a challenge. Paired materials preparation and fabrication processes should also be further optimized for the integration of various sensors and synaptic devices.

For material preparation by bottom-up synthesis/growth methods, paired engineering strategies such as component modulation, doping, and surface modification can be readily used to improve the properties and stability of the materials. The discovery of 2D materials has provided a top-down mechanical exfoliation approach to obtain 2D layered materials. Combining bottom-up stacking/stitching of the layers provides a freely designable solution to device construction. This heterogeneous stacking strategy can also be extended to other dimensional materials to discover more exotic properties, such as quantum dots/2D structures, nanowires/2D structures, organic/2D junctions, etc. In addition, this strategy is compatible with silicon wafer technology and provides a possibility for device size reduction and large-scale preparation by using improved interfacial interactions (e.g., large-area growth and transfer techniques, gold-assisted exfoliation techniques). In addition, the properties of the novel materials can be predicted with the help of software simulation and machine learning.

Device

Currently, most of the sensors are still at macroscopic scale, which is difficult to match with nanoscale synaptic devices. Therefore, it is necessary to address the issues of compatible integration between sensors and synaptic devices in terms of size reduction and signal domain. Meanwhile, how to design the required sensors with high sensitivity, fast response time, good stability, and tunable synaptic properties should be emphatically considered during device fabrication. In addition, in order to realize multimodal sensing and computing, techniques for decoupling multiple singles, designs for innovative device structure, and explanations for new sensing mechanisms are all necessary to be further improved and developed. Besides, considering the interaction with the environment, some irresistible factors (such as noise and other issues) can interfere with the signal from the sensors, making the system less stable and

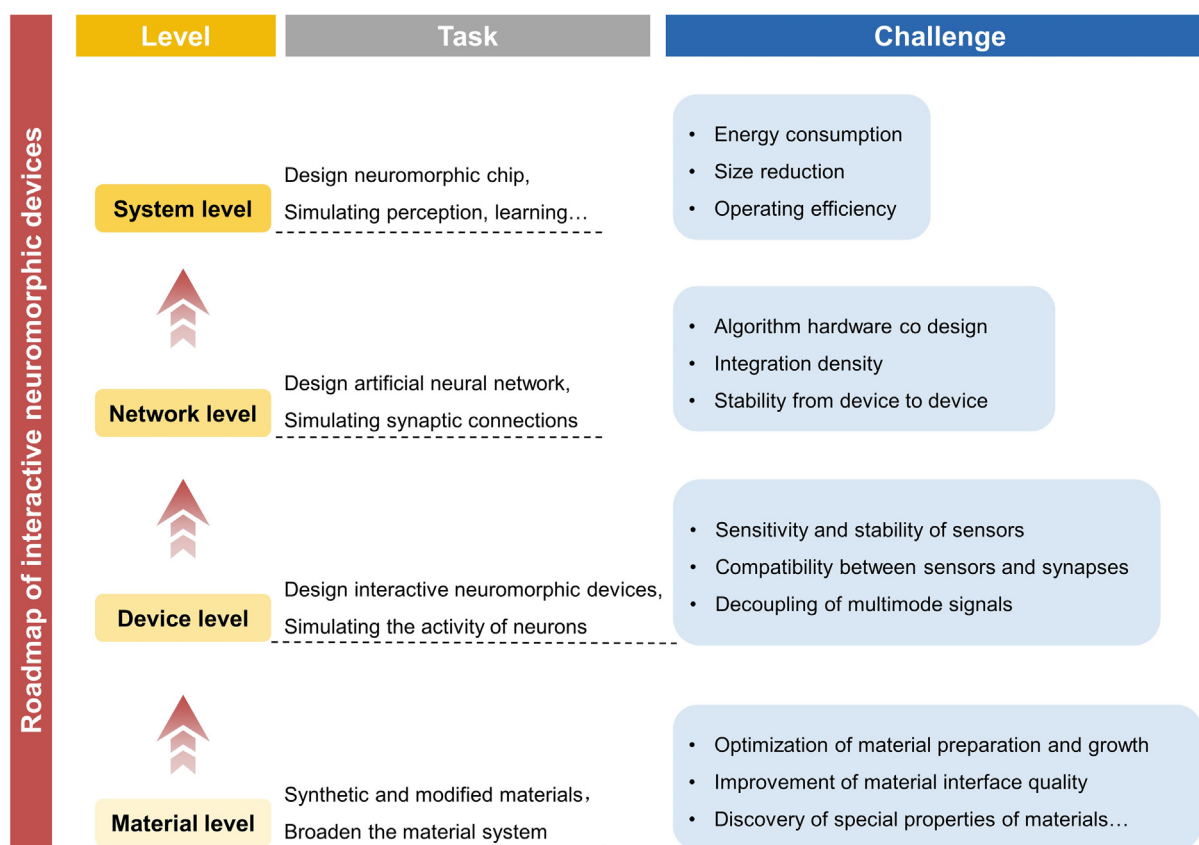


FIGURE 10

Roadmap of bioinspired interactive neuromorphic devices.

reliable. The signal integration problem can be solved by data fusion strategies. Pre-processing of the signal (e.g., data format, dimensionality, sparsity mismatch) can be combined with machine learning and other means to improve the recognition accuracy. The limitation of sensor size makes the system challenging for further integration. One strategy is to continue exploring approaches to reduce the size of sensors and synaptic devices. The complexity of system integration can be simplified by developing devices with new materials, new structures, and new principles that explore the inherent properties of the materials/structures, such as piezoelectric properties, optoelectronic properties, temperature and humidity sensing properties, and chemical sensing properties, to enable in situ detection and signal processing.

Network

From the aspect of neural network, the plasticity of synaptic devices, the linearity and high symmetry of updated conductance, and the stability between devices are the prerequisites for hardware-level artificial synapse arrays to establish highly accurate software-level artificial neural networks and to implement comprehensive solutions to complex and realistic problems. In addition, paired algorithms should be elaborated for specific sensing modes or novel device structures to support more sophisticated neuromorphic computation and patterns recognition.

System

From the aspect of system integration, energy consumption is an everlasting theme with the increased integration level. To solve this problem, how to reduce the power consumption of a single device for the underlying hardware and optimize the neural network architecture and algorithms for software is of great significance.

The proposed bioinspired interactive neuromorphic devices provide solutions to next generation of interactive sensation/memory/computation toward the development of multimodal, low-power, and large-scale intelligent systems endowed with neuromorphic features. Interactive devices/systems embodied neuromorphic intelligence promise to interact with the environments, humans, and robotics more smoothly and adaptively, enabling to construct compact and energy-efficient neuromorphic Internet of Things capable of perceiving, computing, learning, and handling on real-world problems.

Declaration of Competing Interest

The authors declare that they have no known competing financial interests or personal relationships that could have appeared to influence the work reported in this paper.

Acknowledgement

This work is financially supported by the National Key Research and Development Program of China (2021YFB3200304), the National Natural Science Foundation of

China (52073031), China National Postdoctoral Program for Innovative Talents (BX2021302), Beijing Nova Program (Z191100001119047, Z211100002121148), Fundamental Research Funds for the Central Universities (E0EG6801X2), and the “Hundred Talents Program” of the Chinese Academy of Sciences.

References

- [1] A. Demming et al., *Nanotechnology* 24 (2013) 380201.
- [2] J. Backus, *Commun. ACM* 21 (1978) 613–641.
- [3] F.C. Zhou, Y. Chai, *Nat. Electron.* 3 (2020) 664–671.
- [4] T. Wan et al., *Sci. China Inf. Sci.* 65 (2021) 141401.
- [5] H. Tan et al., *Nat. Commun.* 12 (2021) 1120.
- [6] C. Watson et al., *The Brain* (2010) 1–10.
- [7] M. Lee et al., *Adv. Mater.* 29 (2017) 1700951.
- [8] J. Sun et al., *Adv. Funct. Mater.* 28 (2018) 1804397.
- [9] L. Gu et al., *Nature* 581 (2020) 278–282.
- [10] S. Kim et al., *ACS Nano* 11 (2017) 2814–2822.
- [11] L. Mennel et al., *Nature* 579 (2020) 62–66.
- [12] S. Seo et al., *Nat. Commun.* 9 (2018) 5106.
- [13] J. Yu, et al., *Sci. Adv.* 7 (2021), eabd9117.
- [14] F.Y. Liao et al., *Nat. Electron.* 5 (2022) 84–91.
- [15] Z. Ling et al., *Electronics & Packaging* 21 (2021) 060101.
- [16] S.H. Jo et al., *ACS Nano* 10 (2010) 1297–1301.
- [17] S.G. Kim et al., *Adv. Mater. Technol.* 3 (2018) 1800457.
- [18] D. Ielmini, H.S.P. Wong, *Nat. Electron.* 1 (2018) 333–343.
- [19] M. Rahimi Azghadi, et al., *Adv. Intell. Syst.* 2 (2020), 1900189.
- [20] Q. Xia, J.J. Yang, *Nature Mater.* 18 (2019) 309–323.
- [21] S. Choi et al., *Nature Mater.* 17 (2018) 335–340.
- [22] M.A. Zidan et al., *Nat. Electron.* 1 (2018) 22–29.
- [23] Q. Lai et al., *Adv. Mater.* 22 (2010) 2448–2453.
- [24] L. Kergoat et al., *Anal. Bioanal. Chem.* 402 (2012) 1813–1826.
- [25] H. Tian et al., *Nano Lett.* 15 (2015) 8013–8019.
- [26] H. Tian et al., *Nanoscale* 9 (2017) 9275–9283.
- [27] H. Wang et al., *Adv. Mater.* 30 (2018) e1803961.
- [28] J. Zhu et al., *Adv. Mater.* 30 (2018) e1800195.
- [29] Y.H. Chen et al., *Adv. Funct. Mater.* 29 (2019) 1900959.
- [30] L.-A. Kong et al., *Org. Electron.* 47 (2017) 126–132.
- [31] Y. Kim et al., *Science* 360 (2018) 998–1003.
- [32] J. Yu et al., *Nat. Commun.* 12 (2021) 1581.
- [33] D. Ielmini, G. Pedretti, *Adv. Intell. Syst.* 2 (2020) 2000040.
- [34] M. Prezioso et al., *Nature* 521 (2015) 61–64.
- [35] T. Chang et al., *ACS Nano* 5 (2011) 7669–7676.
- [36] M. Hansen et al., *Sci. Rep.* 5 (2015) 13753.
- [37] T. Ohno et al., *Nature Mater.* 10 (2011) 591–595.
- [38] X. Zhu et al., *Nature Mater.* 18 (2019) 141–148.
- [39] W. Xu et al., *Adv. Mater.* 28 (2016) 5916–5922.
- [40] Y. Wang et al., *Adv. Mater.* 30 (2018) e1802883.
- [41] R.A. John et al., *Adv. Mater.* 30 (2018) e1805454.
- [42] H. Tian et al., *ACS Nano* 11 (2017) 12247–12256.
- [43] Y. Wang et al., *Small* 15 (2019) e1805431.
- [44] Y. Zang et al., *Adv. Mater.* 29 (2017) 1606088.
- [45] C. Liu et al., *Nature Nanotechnol.* 15 (2020) 545–557.
- [46] S. Dai et al., *Adv. Funct. Mater.* 29 (2019) 1903700.
- [47] S.H. Kim et al., *Adv. Mater.* 25 (2013) 1822–1846.
- [48] W. Xu et al., *Sci. Adv.* 2 (2016) e1501326.
- [49] G.Y. Gou et al., *J. Mater. Chem. C* 4 (2016) 11110–11117.
- [50] J.T. Yang et al., *Adv. Mater.* 30 (2018) e1801548.
- [51] C.J. Wan et al., *ACS Appl. Mater. Inter.* 8 (2016) 9762–9768.
- [52] J. Jiang et al., *Small* 13 (2017) 1700933.
- [53] Y.L. He et al., *J. Mater. Chem. C* 6 (2018) 5336–5352.
- [54] Y. van de Burgt et al., *Nature Mater.* 16 (2017) 414–418.
- [55] J. Gao et al., *Adv. Funct. Mater.* 32 (2022) 2110415.
- [56] U. Schroeder et al., *Nat. Rev. Mater.* 7 (2022) 653–669.
- [57] Z.D. Luo et al., *ACS Nano* 16 (2022) 3362–3372.
- [58] M.W. Si et al., *Nat. Electron.* 2 (2019) 580–586.
- [59] A.I. Khan et al., *Nat. Electron.* 3 (2020) 588–597.
- [60] T.S. Bösccke, et al., In *2011 International Electron Devices Meeting*, (2011), pp 24.25.21–24.25.24
- [61] C. Ge et al., *Adv. Mater.* 31 (2019) e1900379.
- [62] B.B. Tian et al., *Adv. Electron. Mater.* 5 (2019) 1800600.
- [63] L. Wang et al., *Adv. Funct. Mater.* 30 (2020) 2004609.
- [64] S. Wang et al., *Nat. Commun.* 12 (2021) 53.
- [65] L. Van Tho et al., *Nano Conver.* 3 (2016) 10.
- [66] X.X. Yang et al., *Adv. Funct. Mater.* 30 (2020) 2002506.
- [67] D. Li et al., *Nature Nanotechnol.* 12 (2017) 901–906.
- [68] C. Liu et al., *Nature Nanotechnol.* 13 (2018) 404–410.
- [69] P.F. Wang et al., *Science* 341 (2013) 640–643.
- [70] M. Jia et al., *Sci. Bull.* 67 (2022) 803–812.
- [71] Y. Liu et al., *Nat. Rev. Mater.* 1 (2016) 1.
- [72] H. Tian et al., *ACS Nano* 11 (2017) 7156–7163.
- [73] K. Roy et al., *Nature Nanotechnol.* 8 (2013) 826–830.
- [74] H. Xu et al., *Small* 10 (2014) 2300–2306.
- [75] D. Jariwala et al., *Nature Mater.* 16 (2017) 170–181.
- [76] D. Kufer et al., *Adv. Mater.* 27 (2015) 176–180.
- [77] Y. Ye et al., *J. Mater. Chem.* 21 (2011) 11760–11763.
- [78] J. Heo et al., *Nano Lett.* 13 (2013) 5967–5971.
- [79] P.P. Atluri, W.G. Regehr, *J. Neurosci.* 16 (1996) 5661–5671.
- [80] D.V. Buonomano, W. Maass, *Nat. Rev. Neurosci.* 10 (2009) 113–125.
- [81] L.Q. Zhu et al., *Nat. Commun.* 5 (2014) 3158.
- [82] D.O. Hebb, Wiley: New York, 1949, pp. 335.
- [83] H. Markram et al., *Science* 275 (1997) 213–215.
- [84] G.Q. Bi, M.M. Poo, *J. Neurosci.* 18 (1998) 10464–10472.
- [85] S. Yu, *Proc. IEEE* 106 (2018) 260–285.
- [86] L. Liu, et al., *Nature Nanotechnol.* (2021),
- [87] Z.C. Zhang et al., *Adv. Funct. Mater.* 31 (2021) 2102571.
- [88] W. Zhang et al., *Nat. Electron.* 3 (2020) 371–382.
- [89] I.T. Wang et al., *Nanotechnology* 27 (2016) 365204.
- [90] M. Jerry, et al., In *2017 IEEE International Electron Devices Meeting (IEDM)*, (2017), pp 6.2.1–6.2.4.
- [91] E.A. Lumpkin, M.J. Caterina, *Nature* 445 (2007) 858–865.
- [92] C. Wan et al., *Adv. Mater.* 30 (2018) e1801291.
- [93] S. Sundaram, *Science* 370 (2020) 768–769.
- [94] Y. Lee et al., *Adv. Funct. Mater.* 30 (2020) 1904523.
- [95] Y. Zang et al., *Nat. Commun.* 6 (2015) 6269.
- [96] B.C. Tee et al., *Science* 350 (2015) 313–316.
- [97] H.H. Chou et al., *Nat. Commun.* 6 (2015) 8011.
- [98] S.C. Mannsfeld et al., *Nature Mater.* 9 (2010) 859–864.
- [99] H. Shim, et al., *Sci. Adv.* 5 (2019), eaax4961.
- [100] M. Wang et al., *Adv. Mater.* (2022) e2201962.
- [101] Z.L. Wang, *Adv. Mater.* 24 (2012) 4632–4646.
- [102] C. Pan et al., *Chem. Rev.* 119 (2019) 9303–9359.
- [103] J.R. Yu et al., *Adv. Intell. Syst.* 2 (2020) 1900175.
- [104] S. Zhang et al., *Nat. Commun.* 11 (2020) 326.
- [105] W.B. Ding et al., *Adv. Mater. Technol.* 4 (2019) 1800487.
- [106] C.S. Wu et al., *Adv. Energy Mater.* 9 (2019) 1802906.
- [107] C. Zhang et al., *ACS Nano* 8 (2014) 8702–8709.
- [108] G. Gao et al., *Adv. Mater.* 31 (2019) e1806905.
- [109] X. Yang et al., *ACS Nano* 14 (2020) 8668–8677.
- [110] Y.R. Lee et al., *Nat. Commun.* 11 (2020) 2753.
- [111] X. Liao et al., *Nat. Commun.* 11 (2020) 268.
- [112] Y. Lee, et al., *Sci. Adv.* 4 (2018), eaat7387.
- [113] K. He et al., *Adv. Mater.* 32 (2020) e1905399.
- [114] J.J. Nassi, E.M. Callaway, *Nat. Rev. Neurosci.* 10 (2009) 360–372.
- [115] D. Berco, D. Shenp, *Ang. Adv. Intell. Syst.* 1 (2019), 1900003.
- [116] J. Zhang et al., *Adv. Intell. Syst.* 2 (2020) 1900136.
- [117] Z. Cheng et al., *Sci. Adv.* 3 (2017) e1700160.
- [118] S. Seo et al., *ACS Appl. Electron. Mater.* 2 (2020) 371–388.
- [119] S. Seo et al., *Adv. Mater.* 33 (2021) e2102980.
- [120] H.J. Queisser, D.E. Theodorou, *Phys. Rev. B* 33 (1986) 4027–4033.
- [121] H. Tan et al., *Nano Energy* 52 (2018) 422–430.
- [122] Q.B. Zhu et al., *Nat. Commun.* 12 (2021) 1798.
- [123] C.J. O’Kelly et al., *Adv. Electron. Mater.* 2 (2016) 1500458.
- [124] W. Zhou et al., *Appl. Phys. Lett.* 113 (2018) 061107.
- [125] Y. Meng, et al., *Sci. Adv.* 6 (2020), eabc6389.
- [126] H.K. He et al., *Small* 14 (2018) e1800079.
- [127] R.A. John et al., *Adv. Mater.* 30 (2018) e1800220.
- [128] T. Ahmed et al., *Adv. Funct. Mater.* 29 (2019) 1901991.
- [129] C.Y. Wang, et al., *Sci. Adv.* 6 (2020), eaba6173.
- [130] M. Kumar et al., *Adv. Mater.* 31 (2019) e1900021.
- [131] F. Zhou et al., *Nature Nanotechnol.* 14 (2019) 776–782.
- [132] W. Deng et al., *NPG Asia Mater.* 11 (2019) 77.
- [133] Y.X. Hou et al., *ACS Nano* 15 (2021) 1497–1508.
- [134] Z. Cheng et al., *Adv. Mater.* 30 (2018) e1802435.

- [135] M. Karbalaee Akbari, S. Zhuiykov, *Nat. Commun.* 10 (2019) 3873.
- [136] V.K. Sangwan, M.C. Hersam, *Nature Nanotechnol.* 15 (2020) 517–528.
- [137] S.J. Tans et al., *Nature* 393 (1998) 49–52.
- [138] R. Martel et al., *Appl. Phys. Lett.* 73 (1998) 2447–2449.
- [139] S.H. Chae, Y.H. Lee, *Nano Converg.* 1 (2014) 15.
- [140] B. Tian, C.M. Lieber, *Chem. Rev.* 119 (2019) 9136–9152.
- [141] G. Fiori et al., *Nature Nanotechnol.* 9 (2014) 768–779.
- [142] A.K. Geim, I.V. Grigorieva, *Nature* 499 (2013) 419–425.
- [143] M. Chhowalla et al., *Nat. Rev. Mater.* 1 (2016).
- [144] A. Castellanos-Gomez et al., *Nat. Rev. Meth. Primers* 2 (2022) 1–19.
- [145] Y. Huang et al., *Nat. Commun.* 11 (2020) 2453.
- [146] J. Zhou et al., *Nature* 556 (2018) 355–359.
- [147] J. Qiao et al., *Nat. Commun.* 5 (2014) 4475.
- [148] T. Hong et al., *Nanoscale* 7 (2015) 18537–18541.
- [149] L. Li et al., *Nature Nanotechnol.* 9 (2014) 372–377.
- [150] H. Liu et al., *Adv. Mater.* 30 (2018) e1800295.
- [151] O. Lopez-Sanchez et al., *Nature Nanotechnol.* 8 (2013) 497–501.
- [152] D. Xiang et al., *Nat. Commun.* 9 (2018) 2966.
- [153] Q. Wang, et al., *Sci. Adv.* 4 (2018), eaap7916.
- [154] X. Chen et al., *Adv. Mater.* 32 (2020) 1902039.
- [155] D. De Fazio et al., *ACS Nano* 10 (2016) 8252–8262.
- [156] Y. Wen et al., *Adv. Mater.* 32 (2020) e1906874.
- [157] S. Qin et al., *2D Mater.* 4 (2017) 035022.
- [158] L. Pi et al., *Nat. Electron.* 5 (2022) 248–254.
- [159] X. Wu et al., *Adv. Sci.* 4 (2017) 1700442.
- [160] J. Shi et al., *Adv. Mater.* 34 (2022) e2200380.
- [161] W. Wang, et al., *Sci. Adv.* 4 (2018), eaat4752.
- [162] L. Sun et al., *Nano Lett.* 18 (2018) 3229–3234.
- [163] S. Das et al., *Nat. Commun.* 10 (2019) 3450.
- [164] S. Seo et al., *Nat. Commun.* 11 (2020) 3936.
- [165] S. Oh et al., *Adv. Sci.* 9 (2022) e2103808.
- [166] Y.Q. Liu et al., *Nano Energy* 78 (2020) 105403.
- [167] H.S. Wang, et al., *Sci. Adv.* 7 (2021), eabe5683.
- [168] H.P. Liu et al., *Int. J. Adv. Robot. Syst.* 14 (2017) 1–12.
- [169] H. Wei et al., *Nat. Commun.* 12 (2021) 1068.
- [170] M. Wang et al., *Nat. Electron.* 3 (2020) 563–570.
- [171] X.M. Wu et al., *Nano Energy* 85 (2021) 106000.
- [172] M. Liu et al., *Nat. Commun.* 13 (2022) 79.
- [173] S. Luo et al., *Mechatronics* 48 (2017) 54–67.
- [174] P. Allen, In *Proceedings - IEEE International Conference on Robotics and Automation*, (1984), pp 394-397
- [175] M. Bjorkman et al., *Ieee. Int. C. Int. Robot* (2013) 3180–3186.
- [176] J. Ilonen et al., *Ieee. Int. Conf. Robot* (2013) 3547–3554.
- [177] J.S. Son, et al., In *Proceedings of IEEE/RSJ International Conference on Intelligent Robots and Systems. IROS '96*, (1996), Vol. 3, pp 1068-1075 vol.1063.
- [178] Y. Bekiroglu et al., *Ieee. Int. Conf. Robot* (2013) 3040–3047.
- [179] M. Boshra, H. Zhang, *Pattern Recognit.* 33 (2000) 483–501.
- [180] C. Wan et al., *Nat. Commun.* 11 (2020) 4602.
- [181] S. Furber, *J. Neural Eng.* 13 (2016) 051001.
- [182] Y. LeCun et al., *Nature* 521 (2015) 436–444.
- [183] M.M. Shulaker et al., *Nature* 547 (2017) 74–78.
- [184] M. Kumar et al., *Nano Energy* 73 (2020) 104756.
- [185] Y.Q. Liu et al., *Nano Energy* 60 (2019) 377–384.
- [186] C. Shen et al., *Nanotechnology* 33 (2021) 065205.
- [187] J.L. Meng et al., *Nano Lett.* 22 (2022) 81–89.
- [188] Y. Cheng et al., *Small* 16 (2020) e2005217.
- [189] S. Wang et al., *Natl. Sci. Rev.* 8 (2021) nwaa172.
- [190] Z. Zhang et al., *Nature Nanotechnol.* 17 (2022) 27–32.
- [191] C. Choi et al., *Nat. Commun.* 11 (2020) 5934.
- [192] Z.C. Zhang et al., *Nano Res.* 14 (2021) 4591–4600.
- [193] H.H. Wei et al., *Nano Energy* 81 (2021) 105648.
- [194] D. Berco et al., *Adv. Intell. Syst.* 2 (2019) 1900115.
- [195] H. Tan et al., *Nat. Commun.* 11 (2020) 1369.
- [196] S.Q. Lan et al., *J. Mater. Chem. C* 9 (2021) 3412–3420.